Diminished inhibition and facilitated activation of RyR2-mediated Ca2+ release is a common defect of arrhythmogenic calmodulin mutations

Søndergaard, Mads T; Liu, Yingjie; Brohus, Malene; Guo, Wenting; Nani, Alma; Carvajal, Catherine; Fill, Michael; Overgaard, Michael T; Chen, S R Wayne

Published in:
F E B S Journal

DOI (link to publication from Publisher):
10.1111/febs.14969

Publication date:
2019

Document Version
Accepted author manuscript, peer reviewed version

Received Date : 21-Dec-2018
Revised Date : 23-Apr-2019
Accepted Date : 20-Jun-2019

Diminished inhibition and facilitated activation of RyR2-mediated Ca^{2+} release is a common defect of arrhythmogenic calmodulin mutations

Mads T. Søndergaard[a,b*], Yingjie Liu[b], Malene Brohus[a], Wenting Guo[b], Alma Nani[c], Catherine Carvajal[c], Michael Fill[c], Michael T. Overgaard[a†] and S.R. Wayne Chen[b,c†*]

From the [a]Department of Chemistry and Bioscience, Aalborg University, 9220 Aalborg, Denmark; the [b]Libin Cardiovascular Institute of Alberta, Department of Physiology and Pharmacology and Department of Biochemistry and Molecular Biology, University of Calgary, Calgary, Alberta, T2N 4N1, Canada; and the [c]Department of Molecular Biophysics and Physiology, Rush University Medical Center, Chicago, Illinois 60612, USA

Running Title: CaM mutations diminish inhibition and facilitate activation of RyR2

Article type : Original Article

[*]To whom correspondence should be addressed: Department of Chemistry and Bioscience, Aalborg University, 9220 Aalborg, Denmark. Tel.: 40616849; mts@bio.aau.dk or Libin Cardiovascular Institute of Alberta, Department of Physiology and Pharmacology, HRIC GAC58, 3330 Hospital Dr. N.W., Calgary, AB, Canada. Tel.: 403-220-4235; Fax: 403-270-0313; swchen@ucalgary.ca
[†]co-senior authors.

ABSTRACT

A number of calmodulin (CaM) mutations cause severe cardiac arrhythmias, but their arrhythmogenic mechanisms are unclear. While some of the arrhythmogenic CaM mutations have been shown to impair CaM-dependent inhibition of intracellular Ca^{2+} release through the ryanodine receptor type 2 (RyR2), the impact of a majority of these mutations on RyR2 function is unknown. Here we investigated the effect of 14 arrhythmogenic CaM mutations on the CaM-dependent RyR2 inhibition. We found that all the arrhythmogenic CaM mutations tested diminished CaM-dependent inhibition of RyR2-mediated Ca^{2+} release and increased store-overload induced Ca^{2+} release (SOICR) in HEK293 cells. Moreover, all the arrhythmogenic CaM mutations tested either failed to inhibit or

This article has been accepted for publication and undergone full peer review but has not been through the copyediting, typesetting, pagination and proofreading process, which may lead to differences between this version and the Version of Record. Please cite this article as doi: 10.1111/febs.14969

even promoted RyR2-mediated Ca^{2+} release in permeabilized HEK293 cells with elevated cytosolic Ca^{2+}, which was markedly different from the inhibitory action of CaM wild type. The CaM mutations also altered the Ca^{2+}-dependency of CaM binding to the RyR2 CaM-binding domain. These results demonstrate that diminished inhibition, and even facilitated activation, of RyR2–mediated Ca^{2+} release is a common defect of arrhythmogenic CaM mutations.

Keywords

Ryanodine receptor, calmodulin, arrhythmia, intracellular Ca^{2+} release, protein regulation.

List of abbreviations

Calmodulin (CaM), sarcoplasmic reticulum Ca^{2+} release channel or ryanodine receptor type 2 (RyR2), store-overload induced Ca^{2+} release (SOICR), voltage-gated Na^+ channels ($Na_V1.5$), voltage-gated Ca^{2+} channels ($Ca_V1.2$), sarcoplasmic reticulum (SR), cytosolic free Ca^{2+} concentration ($[Ca^{2+}]_{cyt}$), either long-QT syndrome (LQTS), catecholaminergic polymorphic ventricular tachycardia (CPVT), idiopathic ventricular fibrillation (IVF), calmodulin-binding domain (CaMBD), free Ca^{2+} concentration ($[Ca^{2+}]_{free}$), sarcoplasmic/endoplasmic reticulum Ca^{2+} ATPase 2 (SERCA2b), differences in Gibb's free energies of binding ($\Delta\Delta G^o$), dissociation constant (K_D), free Ca^{2+} concentration required to reach half-saturation of the fluorescence anisotropy Ca^{2+} titration curve (K_{Hill}), calmodulin domain-wise affinity for binding Ca^{2+} ($appK_D$), open probability (P_o), control condition / experiment (Ctrl), mean open time (MOT)
mean closed time (MCT), tritium [^{3}H], Na^+-Ca^{2+}-exchanger (NCX).

Conflicts of interest

The authors declare not to have any actual or potential conflict of interest including any financial, personal or other relationships with other people or organizations within three years of beginning the submitted work that could inappropriately influence, or be perceived to influence, our work.

INTRODUCTION

During cardiac excitation, the opening of voltage-gated Na^+ channels ($Na_V1.5$) in cardiomyocytes results in cell membrane depolarization, which activates voltage-gated Ca^{2+} channels ($Ca_V1.2$). Ca^{2+} entry into the cytoplasm through $Ca_V1.2$ then activates the cardiac sarcoplasmic reticulum (SR) Ca^{2+} release channels (or ryanodine receptor type 2, RyR2) in the SR membrane. The Ca^{2+} released from the SR increases the cytosolic free Ca^{2+} ($[Ca^{2+}]_{cyt}$) throughout the cardiomyocyte and binding of Ca^{2+} to myofilaments results in contraction. Ca^{2+} re-uptake to the SR and extrusion to the extracellular space then returns the cardiomyocyte to resting intracellular Ca^{2+} conditions [1,2].

Calmodulin (CaM) is a cytoplasmic Ca^{2+}-binding protein that strongly influences these excitation-contraction cycles by binding to and regulating other proteins involved in cardiomyocyte Ca^{2+} cycling such as $Na_V1.5$, $Ca_V1.2$ and RyR2 [2]. Mutations in CaM cause severe arrhythmia and sudden cardiac death, most likely due to perturbation of the intricate Ca^{2+} signals required for adequate cardiac excitation-contraction cycles (Figure *1* and Table 1).

Fourteen arrhythmogenic CaM mutations cause severe forms of either long-QT syndrome (LQTS) or catecholaminergic polymorphic ventricular tachycardia (CPVT), and a few mutations can cause both LQTS and CPVT. One mutation, CaM-F90L, causes the less well-defined arrhythmia idiopathic ventricular fibrillation (IVF). LQTS (type 3 and 8) is generally associated with excessive $Na_V1.5$ or $Ca_V1.2$ currents, and CPVT mainly with excessive intracellular Ca^{2+} release through RyR2 [3]. Interestingly, the seven LQTS- or LQTS/CPVT-causing CaM mutations investigated so far (D96V, N98S, D130G, D132H, D132V, E141G and F142L) cause insufficient $Ca_V1.2$ inhibition. However, four of these mutations (N54I, D96V, N98S, D130G and F142L) also cause insufficient inhibition of RyR2 [4-10]. Noteworthy, CaM-F142L is markedly less detrimental to RyR2 regulation, and under some conditions it is even a stronger inhibitor of RyR2 than CaM-WT [6]. Four CaM mutations have been investigated for their effect on $Na_V1.5$, and CaM-E141G reduces CaM's inhibition of the Na^+ current, whereas CaM-D96V and -F142L do not affect regulation of $Na_V1.5$ [8,11]. CaM-D130G also reduces the inhibition of the $Na_V1.5$ Na^+ current, although only observed for a fetal Na_V splice variant [11]. Intuitively, mutations in the Ca^{2+}-sensor CaM are expected to adversely affect the cytoplasmic Ca^{2+} concentration ($[Ca^{2+}]_{cyt}$) dependent regulation of many target proteins, however, this is not always the case and the extent of adverse effects varies [2,4-9,11].

The purpose of this study is to systematically investigate how the arrhythmogenic CaM mutations affect CaM's regulation of RyR2 Ca^{2+} release. Embedded in the SR membrane, RyR2 forms homotetrameric Ca^{2+} channels which CaM binds to stoichiometrically (4 per channel) and CaM generally inhibits RyR2 Ca^{2+} release both at diastole and systole $[Ca^{2+}]_{cyt}$ [2,5,12-15]. CaM has two Ca^{2+} binding domains (N- and C-domain) separated by a flexible linker and each containing two Ca^{2+}-binding EF-hand motifs (Figure *1*) [2,16]. The tripartite interaction between the CaM C-domain, Ca^{2+} and the central CaM-binding domain in RyR2 (CaMBD, RyR2 Arg-3581 to Pro-3607) is essential for CaM's inhibition of RyR2 Ca^{2+} release. Noteworthy, both the CaM N- and C-domain and their binding of Ca^{2+} contribute to the inhibition of RyR2 Ca^{2+} release, although the role of the CaM N-domain is more obscure. It has been proposed that the CaM N-domain may respond to changes in $[Ca^{2+}]_{cyt}$ during cardiomyocyte Ca^{2+} oscillations, and that RyR2 CaMBDs other than the canonical Arg-3581 to Pro-3607 region may be involved in this CaM-dependent RyR2 regulation [2,5,6,12-22].

In this study we investigated the effect on CaM-dependent regulation of RyR2-mediated Ca^{2+} release of fourteen arrhythmogenic CaM mutations. We consider the one N-domain CaM mutation known, N54I, in detail in a separate study [23]. We used single-cell ER luminal Ca^{2+} imaging, single channel recordings, and binding experiments with CaM and a RyR2 CaMBD peptide. We found that these CaM mutations altered the Ca^{2+}-dependency of the CaM-RyR2 CaMBD interaction and generally caused excessive RyR2-mediated Ca^{2+}-release in HEK293 cells as a result of insufficient inhibition of RyR2. Taken together our results support the notion that arrhythmogenic CaM mutations commonly impair CaM-dependent inhibition of RyR2. Our data also reveal that arrhythmogenic CaM mutations can either diminish RyR2 inhibition or even promote RyR2 activation.

RESULTS

Arrhythmogenic CaM mutations reduce CaM-dependent inhibition of RyR2-mediated store-overload induced Ca^{2+} release in HEK293 cells

To investigate the effects of arrhythmogenic CaM mutations on RyR2 inhibition, we monitored store overload induced Ca^{2+} release (SOICR) in RyR2-expressing HEK293 cells co-transfected with the D1ER Ca^{2+} probe and each CaM mutant (Table 2). Perfusion of cells with 2 mM extracellular Ca^{2+} increased the endoplasmic reticulum (ER) free Ca^{2+} concentration (ER Ca^{2+} load) and elicited SOICR such that ER Ca^{2+} load oscillated with the concerted opening and closing of RyR2 channels (see details in 'Experimental procedures' and Figure 2). The activation threshold (the ER Ca^{2+} load at which SOICR initiated) and the termination threshold (the ER Ca^{2+} load at which Ca^{2+} release ceased) were determined using the oscillating D1ER FRET signal in single cells, and the difference (activation threshold – termination threshold) was the fractional ER Ca^{2+} release [5,6,13,24]. An increase in the activation threshold indicates that RyR2 channels are less sensitive to stimulation by ER luminal Ca^{2+}, and an increase in the termination threshold indicates that channels are more susceptible to inactivation once opened. Hence, inhibition of RyR2 Ca^{2+} release increases the activation and/or the termination threshold.

In this experiment we quantified and compared the effects on RyR2 Ca^{2+} release of CaM-WT and ten mutants during SOICR. We previously characterised the five CaM mutations (N54I, D96V, N98S, D130G and F142L) in equivalent experiments [5,6]. The effects of CaM-WT and mutants were quantified relative to the control condition (Ctrl) without CaM transfection (i.e. with only endogenous CaM-WT present) (Figure 3 and Table 2). The recombinant expression of CaM-WT increased the termination threshold 3.4 % and thereby decreased the fractional ER Ca^{2+} release by 3 %. Note that the percentages refer to the unit used for ER Ca^{2+} load, and not relative changes in values. Albeit subtle, the inhibitory effect of CaM-WT on RyR2 Ca^{2+} release is consistently observed across several studies [5,6,13], and a subtle effect was also expected given that HEK293 cells endogenously express CaM. A slight but non-significant increase in the CaM protein level in HEK293 cells transfected with

the CaM-WT plasmid was detected using western blotting (see Figure 9 in 'Experimental procedures'), despite the subtle effect of expression being detectable on the regulation of RyR2 Ca^{2+} release. However, plasmid expression of the other ten CaM variants increased their protein levels 1.8-fold (+/- 0.3), compared to the control and CaM-WT expression, without significant differences among these CaM mutants. The lower protein expression level of CaM-WT could cause an underestimation of the effect of CaM-WT expression, compared to the effects of expressing mutant CaMs. However, any such underestimation would consequently lead to an underestimation of the observed differences between the effects of expressing CaM-WT and the mutant variants, because expression of CaM-WT increased RyR2 inhibition while mutant CaM variants oppositely diminished inhibition. Hence, the validity of the observed differences would increase, if the effect of expressing CaM-WT was underestimated.

Opposite to CaM-WT, the ten CaM mutations tested here all impaired CaM-dependent RyR2 inhibition primarily by decreasing the termination threshold by 17 % on average and increasing the fractional ER Ca^{2+} release by an average 15 % (Figure 3 and Table 2). However, there were noteworthy differences in the extent to which these CaM mutations affected RyR2-mediated Ca^{2+} release (Figure 3). CaM-A103V slightly decreased the termination threshold by 4 % which was opposite to the 3.4 % increase conferred by CaM-WT (Figure 3B, group a). More noticeably, the five CaM mutations D132E, D132H, D132V, D134H and E141G (Figure 3B, group c) strongly decreased the termination threshold by an average 21 % and increased the fractional ER Ca^{2+} release by 20 %. In comparison, a RyR2 variant with the CaMBD deleted (RyR2-ΔCaMBD) is insensitive to regulation by CaM, and this causes a 23 % decrease in the termination threshold and a 23 % increase in fractional ER Ca^{2+} release [5,13]. Thus, partially replacing endogenous CaM-WT with one of the latter five mutants nearly abolished CaM-dependent RyR2 inhibition. Less severe, the three CaM mutations F90L, N98I and D130V (Figure 3B, group b) also markedly lowered the termination threshold by 11 % on average and increased the fractional ER Ca^{2+} release by 10 %. The effect of the CaM mutation Q136P (Figure 3B, group *) was intermediate to those of the severe (c) and less severe (b) mutations, and still markedly lowered the RyR2 termination threshold and increased fractional ER Ca^{2+} release. Interestingly, three of the CaM mutations, CaM-N98I, -D132E and -Q136P, slightly decreased the activation threshold, on average by 4 % (Figure 3A), which indicated that RyR2 channels with either of these CaM mutants bound were slightly more sensitive to SOICR. By comparison, CaM-WT does not significantly affect the activation threshold.

The diminished inhibition of RyR2 Ca^{2+} release during SOICR conferred by the nine CaM mutations (other than A103V) was very similar to that previously observed for the mutations N54I, D96V, N98S and D130G (Table 2) [5]. Specifically, these mutations also lowered the termination threshold by 17 % on average, lowered the activation threshold by 5 % and increased the fractional

ER Ca^{2+} release by 12 %, compared to the control condition. In comparison, CaM-F142L is less detrimental to RyR2 regulation during SOICR which is reminiscent to the effect seen here for CaM-A103V [6].

Arrhythmogenic CaM mutations abolish CaM-dependent inhibition of RyR2-mediated Ca^{2+} release in permeabilized HEK293 cells with elevated cytosolic Ca^{2+}

Ca^{2+} binding to CaM increases its inhibitory effect on RyR2, and CaM bound to RyR2 CaMBD is unlikely to become fully saturated with Ca^{2+} until $[Ca^{2+}]_{cyt}$ is well above 1 μM [2,5,6]. In intact HEK293 cells, $[Ca^{2+}]_{cyt}$ oscillates between approximately 0.05 – 2 μM during SOICR and therefore only briefly exceeds 1 μM [25,26]. Thus, to investigate CaM-dependent RyR2 inhibition under conditions of elevated $[Ca^{2+}]_{cyt,}$ we used permeabilized HEK293 cells and a Ca^{2+}-buffered perfusion medium with a constant free Ca^{2+} concentration ($[Ca^{2+}]_{free}$) of 1 μM.

Endogenous CaM was washed away using prolonged perfusion with a low Ca^{2+} buffer during cell permeabilization. Noteworthy, the cytosolic 1 μM $[Ca^{2+}]_{free}$ strongly activated RyR2 and consequently reduced the ER Ca^{2+} load required for triggering SOICR, i.e. lowered the activation threshold. Under these conditions, RyR2 Ca^{2+} release does not cause oscillations in ER Ca^{2+} concentrations, and instead the ER Ca^{2+} load reaches a steady-state that likely reflects an equilibrium between the opposing fluxes of RyR2 Ca^{2+} release and the SR/ER Ca^{2+} ATPase (SERCA2b) Ca^{2+} uptake [27]. In this setting, any inhibition of RyR2 Ca^{2+} release increases the steady-state ER Ca^{2+} load because ER Ca^{2+} efflux is reduced, while ER Ca^{2+} uptake remains similar. The D1ER FRET signal was used for measuring the steady-state ER Ca^{2+} load in single cells under three different CaM conditions: in the absence of CaM, in the presence of an arrhythmogenic CaM mutation, and in the presence of CaM-WT (Figure 4). The effects of purified CaM-WT and each CaM mutant on RyR2-mediated Ca^{2+} release in permeabilized cells were determined by measuring the difference in steady-state ER Ca^{2+} load without CaM and after addition of each CaM variant, all in the presence of 1 μM cytosolic $[Ca^{2+}]_{free}$ (Figure 5A, and Table 3).

In the presence of 1 μM cytosolic $[Ca^{2+}]_{free}$, addition of exogenous CaM-WT to the permeabilized, RyR2-expressing HEK293 cells on average increased ER Ca^{2+} load by 13 % compared to perfusion with no CaM present. This response indicated the presence of CaM-dependent inhibition of RyR2-mediated Ca^{2+} release even when RyR2 is stimulated by 1 μM cytosolic $[Ca^{2+}]_{free}$. Like the experiments with intact HEK293 cells, the percentages given refer to the unit used for ER Ca^{2+} load. Addition of CaM-F90L, -D96V, -A103V or -F142L (Figure 5A, group a) to permeabilized cells did not significantly inhibit RyR2 Ca^{2+} release compared to the condition without CaM present. In contrast, these CaM mutations seemed to slightly enhance RyR2 Ca^{2+} release (i.e. a decrease in

steady-state ER Ca^{2+} load). This result could not be explained by the lack of CaM binding to RyR2 as they clearly did so in intact HEK293 cells, in protein-peptide binding (see below) and in single channel experiments [5,6]. Hence, it appeared that these mutations, F90L, D96V, A103V and F142L, abolished CaM's ability to inhibit RyR2 under conditions of elevated $[Ca^{2+}]_{cyt}$. Most strikingly, however, ten CaM mutants not only failed to inhibit ER Ca^{2+} release but caused a marked decrease in the steady-state ER Ca^{2+} load compared to the perfusion condition without CaM. The eight CaM mutations N98I, D130G, D130V, D132E, D132H, D132V, D134H and Q136P (Figure 5A, group b) on average caused a 12 % decrease, and the two mutations N98S and E141G (Figure 5A, group *) had a slightly smaller effect on CaM-dependent RyR2 inhibition causing an average 8 % decrease. Therefore, these ten arrhythmogenic CaM mutations (N98I, N98S, D130G, D130V, D132E, D132H, D132V, D134H, Q136P and E141G) seemingly reversed the action of CaM on RyR2 under conditions of sustained 1 μM cytosolic $[Ca^{2+}]_{free}$.

Noteworthy, the effect of CaM on steady-state ER Ca^{2+} was directly related to CaM-dependent regulation of RyR2, because no effect on ER Ca^{2+} was observed when adding CaM to the RyR2-ΔCaMBD variant (Figure 5B). Moreover, cells expressing RyR2 or RyR2-ΔCaMBD reach the same steady-state ER Ca^{2+} with 1 μM cytosolic $[Ca^{2+}]_{free}$ in the absence of CaM which together with the CaM-RyR2 dissociation kinetics support a complete removal of endogenous CaM-WT during the permeabilization process [21,28].

Arrhythmogenic CaM mutations alter the Ca^{2+}-dependency of the interaction between CaM and the RyR2 CaM-binding domain

In order to measure the affinity of CaM variants for binding to the RyR2 CaMBD at physiologically relevant $[Ca^{2+}]_{free}$ (~0.05 – 400 μM) [14,29,30], we titrated a fluorescently labelled peptide (RyR2(R3581-L3611)) with CaM in a $[Ca^{2+}]_{free}$-buffered solution. The binding of CaM to RyR2(R3581-L3611) was monitored using the resulting change in the fluorescence anisotropy (FA) of the peptide and the titration curves, at each fixed $[Ca^{2+}]_{free}$, were fitted to a stoichiometric binding model [31]. This procedure gave the affinity of CaM for binding to RyR2(R3581-L3611) expressed as the interaction's dissociation constant (K_D) as a function of $[Ca^{2+}]_{free}$ (Figure 6**A-C**). A low K_D equates to extensive protein-peptide complex formation and thus a high-affinity interaction. Besides the measured K_D values, the changes in CaM's affinity for binding to RyR2(R3581-L3611) conferred by the CaM mutations were also quantified as the differences in Gibb's free energies of binding ($\Delta\Delta G^o$), comparing to that of the CaM-WT (Figure 6D).

These serial titration curve analyses showed that CaM-WT even without Ca^{2+} (< 0.3 nM $[Ca^{2+}]_{free}$), bound to RyR2(R3581-L3611) with moderate affinity (K_D 1.4 μM) and that the CaM-RyR2(R3581-L3611) interaction was extremely $[Ca^{2+}]_{free}$ -dependent (very steep decline in K_D as

function of $[Ca^{2+}]_{free}$) with the K_D decreasing approximately 1200-fold to 1.1 nM over the $[Ca^{2+}]_{free}$ range 0.01 to 10 μM. In the presence of RyR2(R3581-L3611) both the N- and C-domain of CaM-WT are fully Ca^{2+}-bound at 10 μM $[Ca^{2+}]_{free}$ and above, and no further increase in affinity with increasing $[Ca^{2+}]_{free}$ was observed above 10 μM $[Ca^{2+}]_{free}$ [5,31,32]. All arrhythmogenic CaM mutants retained a moderate affinity for binding to the RyR2 CaMBD both without Ca^{2+} (K_D 1 to 2 μM), and also showed high affinity binding with 10 μM $[Ca^{2+}]_{free}$ (K_D 1 to 8 nM). Noteworthy, above 100 μM $[Ca^{2+}]_{free}$ there were no significant effects of any of the mutations on CaM's affinity for binding to RyR2(R3581-L3611). This indicated that upon saturation with Ca^{2+}, all CaM mutants bound to the peptide with a very high affinity (~1 nM), indistinguishable from that of the CaM-WT. Interestingly, CaM-D132H, -D132V and -E141G displayed a decreased affinity for binding to RyR2(R3581-L3611) in the absence of Ca^{2+} ($\Delta\Delta G^o$, on average 1 kJ/mol). This supported that arrhythmogenic mutations can affect the CaM-RyR2 CaMBD interaction independent of their effect on CaM's affinity for Ca^{2+}, as also shown previously for CaM-D96V and -N98S using isothermal titration calorimetry [6]. Oppositely, CaM-F142L showed a slight increase in affinity for binding to RyR2(R3581-L3611) in the absence of Ca^{2+} which also was consistent with isothermal titration calorimetry measurements [6].

All CaM mutants displayed a pronounced rightward shift in their K_D as a function of $[Ca^{2+}]_{free}$ (Figure 6**A-C**). Consequently, the arrhythmogenic CaM mutants showed markedly decreased affinities for binding to RyR2(R3581-L3611) to various extents across the physiologically relevant $[Ca^{2+}]_{free}$ range, around 0.05 – 200 μM (Figure 6D). Even though the arrhythmogenic mutations lowered CaM's affinity for binding to RyR2 CaMBD at resting Ca^{2+} concentrations (0.05 μM), compared to CaM-WT, they still retained a substantial affinity (K_D 0.6 to 1.7 μM). Thus, our results support that under physiological cell conditions with an excess of target protein binding sites relative to CaM molecules, each of the arrhythmogenic CaM mutants could bind RyR2 CaMBD not occupied by CaM-WT, although they are not able to directly outcompete CaM-WT for binding to RyR2 at any Ca^{2+} concentration [21,33,34]. The results also support that all the arrhythmogenic CaM mutations lower the extent of Ca^{2+} saturation of CaM bound to RyR2 specifically in the $[Ca^{2+}]_{free}$ range corresponding to resting cardiomyocyte conditions and up to approximately 100 μM $[Ca^{2+}]_{cyt}$ [14,29,30].

Arrhythmogenic CaM mutations impair Ca^{2+} binding to CaM in complex with the RyR2 CaM-binding domain

The titration of RyR2(R3581-L3611) with CaM clearly showed that for all CaM mutants their affinity for binding to the peptide was orders of magnitude higher when Ca^{2+} is present. This is consistent with CaM binding to CaMBD and Ca^{2+} binding to CaM being thermodynamically coupled [5,32,35-37], and enabled an estimation of CaM's affinity for binding to Ca^{2+} when complexed with

RyR2(R3581-L3611), i.e estimating CaM's sensitivity to Ca^{2+} when already bound to RyR2 CaMBD [5,6,31]. To this end, the FA measurements for the titration of CaM and peptide at constant concentrations (fixed ratio) with Ca^{2+} were extracted from the larger titration data sets (Figure 7A). These Ca^{2+} titration curves were fitted to an empirical Hill model of Ca^{2+}-binding where the CaM/RyR2(R3581-L3611) complexes' affinities for Ca^{2+} were expressed as the $[Ca^{2+}]_{free}$ required to reach half-saturation of the FA Ca^{2+} titration curve (K_{Hill}).

The K_{Hill} for CaM-WT with RyR2(R3581-L3611) was by this estimation 0.09 μM, and all the arrhythmogenic mutations severely impaired Ca^{2+} binding to the CaM/RyR2(R3581-L3611) complexes (Figure 7B and Table 4). The severity of the effect of CaM mutations on K_{Hill} varied considerably with changes ranging from 3- to 11-fold. The greatest changes (6- to 9-fold, Figure 7B group b) were seen for the eight mutations D130G, D130V, F90L, D132H, D132V, D134H, Q136P and E141G. A significantly smaller effect was observed for the four mutations N98I, N98S, A103V and F142L (3- to 4-fold, Figure 7B group a), and finally effects of intermediate magnitude were observed for CaM-D96V and -D132E (5- to 6-fold, Figure 7B group *). These results supported that even when bound to the RyR2 CaMBD, the arrhythmogenic CaM mutants were considerably less prone to binding Ca^{2+} than the CaM-WT. Moreover, the Ca^{2+} titration results also indicated that highly variable $[Ca^{2+}]_{cyt}$ concentrations are required to saturate all the CaM Ca^{2+} binding sites of the CaM/CaMBD complexes with arrhythmogenic CaM mutations present.

Of note, the Ca^{2+} affinity estimation in this study represents a composite of the Ca^{2+} binding affinities of either CaM domain and gives a K_{Hill} which is intermediate of the CaM domain-wise affinity for binding Ca^{2+} ($appK_D$) obtained using intrinsic protein fluorescence [6]. Moreover, the fluorescence anisotropy method of estimating K_{Hill} is biased towards the affinity of the CaM domain that binds Ca^{2+} at the lowest $[Ca^{2+}]_{free}$ (natively the C-domain), as seen from comparing K_{Hill} to $appK_D$ in Table 4.

Arrhythmogenic CaM mutations in the C-domain EF-hand interface show highly diverse effects on the regulation of single RyR2 channels

We have previously shown that CaM-F142L in single RyR2 channel experiments decreased RyR2 open probability (P_o) even more so than the CaM-WT, despite that the F142L mutation strongly reduces CaM's affinity for binding to Ca^{2+} [6]. On the other hand, CaM-D96V, -N98S, -D130G bound to single RyR2 channels, but failed to decrease the P_o. One potential explanation for these differences may be the distinct locations of the mutations as judged by the protein crystal structures of Ca^{2+}-bound CaM (e.g. PDB files **2BCX**, **1CLL**, **1CFF**, **2F3Y**, **6GDK**, **6DAF**) [10,38-41]. The F142L mutation is located at the interface between EF-hand 3 and 4 in the CaM C-domain, whereas the other

CaM C-domain mutations are located at Ca^{2+}-coordinating residues in the EF-hand loops and not part of the EF-hands' interface (Figure 8A).

Interestingly, the mutations F90L and A103V are also located at the interface between EF-hand 3 and 4, and markedly shifted the Ca^{2+}-dependency of the CaM-RyR2(R3581-L3611) interaction (Figure 6D). Yet their detrimental effects on CaM-dependent RyR2 inhibition were less severe compared to the other mutations (Figure 3B and Figure 5A). Hence, we speculated that CaM mutations at the EF-hand 3 and 4 interface not only affect CaM's Ca^{2+} binding and but also cause structural perturbations different from those at the Ca^{2+}-coordinating sites, and that these perturbations in the CaM-RyR2 CaMBD interaction give a less straightforward correlation between decreased Ca^{2+} affinity and effect on CaM-dependent RyR2 regulation.

To explore this notion further we tested the effect of CaM-F90L, -A103V and -Q136P mutations, located at the interface, on the activity of single RyR2 channels in lipid bilayers with 10 μM cytosolic Ca^{2+} (Figure 8B-D and Table 5). It is worth recapitulating that RyR2 Ca^{2+} release and its CaM-dependent inhibition both are processes strongly depend on Ca^{2+} concentrations [2,15,42], and the three functional RyR2 experiments in this study represent three distinct conditions: 1) 0.05 – 2 μM oscillating $[Ca^{2+}]_{cyt}$ in intact HEK293 cells, 2) 1 μM $[Ca^{2+}]_{cyt}$ in permeabilized cells, and 3) 10 μM $[Ca^{2+}]_{cyt}$ for single RyR2 channel experiments. Noteworthy, using 10 μM $[Ca^{2+}]_{free}$ in permeabilized HEK293 cells is not feasible because the strong stimulation of RyR2 by cytosolic Ca^{2+} makes the effect of adding CaM undetectable in that particular setting.

Single RyR2 channel activities were measured before and after the addition of 1 μM of either CaM-WT, -F90L, -A103V or -Q136P, in the presence of 1 mM luminal and 10 μM cytosolic Ca^{2+}. Channel recordings in the absence of CaM were used as the control condition (Ctrl). Addition of CaM-WT to the cytosolic side significantly lowered the RyR2 channel open probability (P_O) from 0.42 to 0.23, compared to the control (i.e. without CaM) (Figure 8B). The mean open time (MOT) decreased from 5.5 to 2.7 ms (Figure 8B) and the mean closed time (MCT) increased from 7.2 to 9.7 ms (Figure 8C) after the addition of CaM-WT, although only the effect on MOT, but not on MCT, was statistically significant compared to the control. This effect of CaM-WT on RyR2 single channels was consistent with previous results [6].

Similar to CaM-WT, CaM-F90L lowered the RyR2 P_o by decreasing the MOT and increasing the MCT, as compared to the control, although the effect on MCT was not statistically significant. CaM-F90L appeared to cause a slightly lower decrease in Po and MOT than that conferred by the CaM-WT. However, single RyR2 channels measured in the presence of CaM-F90L were not significantly

different from those measured with CaM-WT. I.e. CaM-F90L appeared to inhibit single RyR2 channels with 10 μM cytosolic Ca^{2+} very similarly to the CaM-WT. On the other hand, CaM-A103V affected RyR2 regulation nearly opposite to the action of CaM-WT. CaM-A103V markedly increased RyR2 P_o from 0.23 to 0.78, compared to the CaM-WT addition, and did so by both increasing MOT from 2.7 to 12 ms, and decreasing MCT from 9.7 to 3.6 ms. Moreover, CaM-A103V increased RyR2 P_o to well above the activity level observed without CaM (P_o 0.78 vs 0.47) which indicated that CaM-A103V facilitated the activation of single RyR2 channels in stark contrast to the native inhibitory role of CaM-WT. Interestingly, CaM-Q136P showed an action similar to CaM-A103V, although to a lesser extent. Addition of CaM-Q136P increased RyR2 Po from 0.23 to 0.57, compared to the addition of CaM-WT, and did so also by lowering RyR2 MCT from 9.7 to 4.3 ms. CaM-Q136P also slightly increased RyR2 MOT from 2.7 to 6.8 ms, although there was no significant difference when comparing to the control. Thus, these data suggest that arrhythmogenic CaM mutations located at the interface between EF-hands 3 and 4 in the CaM C-domain exert a complex effect on single RyR2 channel gating.

DISCUSSION

Recent studies show that some arrhythmogenic CaM mutations affect the regulation of RyR2. Hwang et al. found that CaM-N54I and -N98S, but not CaM-D96V, diminished CaM's inhibition of single RyR2 channels and promoted spontaneous Ca^{2+} waves in permeabilized rat ventricular myocytes [7]. Nomikos *et al.* and Vassilakopoulou *et al.* found that CaM-N54I, -D96V, -F90L and -D130G increased [^{3}H]-ryanodine binding (a measure of RyR2 open propensity) to porcine cardiac SR vesicles [43-45]. We previously found that CaM-N54I, -D96V, -N98S and -D130G markedly diminished CaM-dependent inhibition of RyR2-mediated SOICR in HEK293 cells and, to a noticeably smaller degree, so did CaM-F142L. Also, CaM-N54I, -D96V, -N98S and -D130G inhibited RyR2 single channels with 10 μM cytosolic Ca^{2+} less so than CaM-WT while CaM-F142L was a stronger inhibitor than CaM-WT [5,6].

In this study we investigated the effect of another ten arrhythmogenic CaM mutations on the regulation of RyR2-mediated Ca^{2+} release during SOICR, and also the effect of all fourteen mutations on CaM-dependent inhibition of RyR2 Ca^{2+} release in permeabilized HEK293 cells with 1 μM cytosolic Ca^{2+}. Our results clearly showed that all ten mutations, to various extents, diminished CaM's inhibition of RyR2-mediated SOICR (Figure 3 and Table 2). Three mutations affected the RyR2 activation threshold for SOICR (CaM-N98I, -D132E and -Q136P) which was similar to that previously observed for CaM-N54I, -N98S, -D96V and -D130G, and supports the notion that these mutations can promote spontaneous Ca^{2+} release in cardiomyocytes during diastole [5,6,42,46-48]. Moreover, all of the fifteen CaM mutations investigated here and previously, impaired termination of

RyR2 Ca^{2+} release which supports that the arrhythmogenic mutations can cause excessive Ca^{2+} release due to diminished inhibition of RyR2 during cardiomyocyte stimulation [20,49]. Interestingly, the five mutations in the CaM EF-hand 4 Ca^{2+} coordinating residues D132, D134 and E141 (Figure *1*), caused a near complete loss-of-function with regard to CaM's role in facilitating the termination of RyR2 Ca^{2+} release [13]. Any of these five mutants (CaM-D132E, -D132V, -D132H, -D134H, -E141G) lowered the RyR2 termination threshold to the same extent observed for the RyR2-ΔCaMBD channel which does not bind CaM. However, absence of CaM binding to RyR2 cannot explain this observation because the CaM mutants clearly bound to RyR2 in permeabilized HEK293 cells, and also bind to the RyR2(R3581-L3611) peptide with appreciable affinity (K_D 1 to 1.8 μM at 0.05 μM $[Ca^{2+}]_{free}$). Also, endogenous CaM-WT would likely mask the effect of a CaM mutant not binding to RyR2 in intact HEK293 cells. Noteworthy, CaM-F142L and -A103V showed considerably less effect on CaM-dependent RyR2 regulation than other mutations with similarly decreased Ca^{2+} binding, and we previously found that CaM-F142L likely has a unique RyR2-CaMBD interaction that may partially compensate for its loss-of-function in terms of CaM binding Ca^{2+} [6].

The results from SOICR experiments in intact HEK293 cells support that the CaM mutations were particular detrimental for the regulation of RyR2 during Ca^{2+} release as opposed to before RyR2 stimulation. Therefore we used permeabilized HEK293 cells to probe CaM-dependent RyR2 regulation during elevated 1 μM $[Ca^{2+}]_{cyt}$ conditions and sustained ER Ca^{2+} release (Figure 5). CaM-WT was a potent inhibitor of RyR2 Ca^{2+} release under these conditions, substantially increasing steady-state ER Ca^{2+} load.This effect of CaM-WT is consistent with CaM's role of inhibiting RyR2 Ca^{2+} release by increasing the termination threshold during SOICR in intact cells [5,6,13]. Remarkably, the fourteen arrhythmogenic CaM mutants tested all failed to inhibit RyR2 Ca^{2+} release at 1 μM sustained cytosolic Ca^{2+}, and ten CaM mutations even increased RyR2 Ca^{2+} release in direct opposition to CaM-WT.

The molecular details of CaM-dependent RyR2 regulation remain unclear. Both CaM domains and their binding of Ca^{2+} contribute to the inhibition of RyR2, and specifically Ca^{2+} binding to the CaM C-domain and binding to the RyR2 CaMBD is a critical interaction for RyR2 regulation [2,5,6,12-22]. The Ca^{2+}-dependent titration of the RyR2(R3581-L3611) peptide with CaM showed that the arrhythmogenic mutations conferred a decreased affinity for binding to the RyR2 CaMBD (Figure 6). This decrease was most pronounced in the Ca^{2+} range corresponding to cardiomyocyte diastole $[Ca^{2+}]_{cyt}$ (~0.1 μM) and early systole (< 10 μM) [14,29,30]. Estimations of CaM mutant affinities for binding to Ca^{2+} in the presence of the RyR2(R3581-L3611) peptide also showed that their CaM C-domains only become Ca^{2+}-saturated at Ca^{2+} concentrations substantially higher than the diastolic $[Ca^{2+}]_{cyt}$ (K_{Hill} 0.3 – 0.8 μM). In contrast, the CaM-WT C-domain is nearly saturated with

Ca^{2+} at 0.1 μM $[Ca^{2+}]_{free}$ [5]. Taken together, these results support the notion that the CaM mutants all can bind to the RyR2 CaMBD, but most likely their CaM C-domains bind in a less Ca^{2+}-saturated state, compared to the native CaM-WT-RyR2 CaMBD interaction, at cardiomyocyte resting conditions and during early systole. We previously proposed that binding of the CaM C-domain to the RyR2 CaMBD in a non-Ca^{2+} saturated condition diminishes CaM-dependent inhibition of RyR2, compared to a Ca^{2+}-bound CaM C-domain [5,6]. This view is supported by the observations that RyR2 association with engineered CaM variants that are deficient in C-domain Ca^{2+}-binding, cause excessive Ca^{2+} release by activating RyR2, and CaM without bound Ca^{2+} is a known agonist of the skeletal muscle SR Ca^{2+} release channel (RyR1) [12,13,15]. Our results here further support this hypothesis for even more CaM mutations, and also demonstrate that a pathological CaM-RyR2 interaction can even facilitate RyR2 Ca^{2+} release, i.e. in addition to causing diminished inhibition of RyR2.

On the other hand, deficiencies in Ca^{2+} binding is not the only determinant of CaM mutation effect on RyR2 regulation, most notable exceptions are CaM-N54I and -F142L [5,6]. The results of single RyR2 channel experiments show that the large CaM Ca^{2+} binding deficiency caused by the F90L mutation does not significantly diminish RyR2 inhibition at 10 μM cytosolic Ca^{2+}, somewhat similar to the F142L mutation (Figure 6D, Figure 8, Table 4 and Table 5). Equally interesting, CaM-A103V and -Q136P are the first arrhythmogenic CaM mutations investigated to cause activation of single RyR2 channels. Thus, CaM-A103V is more detrimental to single RyR2 channel regulation (increases P_o) than CaM-D96V and -D130G (fail to lower P_o) despite showing much less perturbation of CaM Ca^{2+} binding properties [50,51]. Similarly, CaM-Q136P also facilitates single RyR2 channel opening while decreasing CaM's Ca^{2+} binding approximately to the same extent observed for CaM-D130G [50,52].

Generally, it appears that discrepancies between a mutation's effect on CaM Ca^{2+} binding and its effect on CaM-dependent RyR2 regulation are most pronounced for mutations of residues that contribute to CaM intramolecular contacts (F90, A103, F142), compared to those that affect Ca^{2+} coordinating residues (D95, N98, D130, D132, D134 and E141), (Figure *1* and Figure 8A). One hypothesis is that CaM mutations affecting intramolecular contacts not only alter CaM's Ca^{2+} binding but also cause significant structural perturbations in the CaM C-domain, and by extension the CaM-RyR2 interaction, and therefore affect CaM-dependent RyR2 regulation in a complex manner. On the other hand, mutations of Ca^{2+} coordinating residues affect primarily CaM Ca^{2+} binding and cause a none-native binding of Ca^{2+}-unsaturated CaM C-domain to the RyR2 CaMBD, which is likely the underlying cause for their diminished inhibition of RyR2. Investigating this hypothesis further will require CaM-RyR2 structural insights which are outside the scope of this study.

Experiments with RyR2-expressing HEK293 cells approximate diastole- and early systole-like Ca^{2+} conditions in cardiomyocytes and have repeatedly proven a valid model for investigating perturbations of cardiomyocyte intracellular Ca^{2+} release [24,46,48,49,53,54]. One reason is that cardiac Ca^{2+}-cycling requires tightly controlled Ca^{2+} homeostasis and even small perturbations to RyR2 Ca^{2+} release can cause severe disease [2,55-57]. Taken together, our results indicate that all the fourteen CaM mutations investigated cause increased SOICR activation and/or excessive Ca^{2+} release through RyR2, albeit to various extents depending on cytosolic Ca^{2+} concentrations. The general mechanism for the excessive Ca^{2+} release appears to result from a severely diminished ability of CaM to inhibit RyR2-mediated Ca^{2+} release once it is activated. Our data indicate that the diminished inhibition of RyR2, as conferred by the arrhythmogenic CaM mutations, is most detrimental near 1 μM, is slightly less severe at 10 μM $[Ca^{2+}]_{cyt}$, and may become negligible for $[Ca^{2+}]_{cyt}$ well above 10 μM.

Assuming that our results hold true in cardiomyocytes, the diminished inhibition of RyR2 caused by arrhythmogenic CaM mutations would most likely occur during early systole of the cardiac cycle, and again during SR Ca^{2+} replenishing as $[Ca^{2+}]_{cyt}$ is brought down to diastole levels. In cardiomyocytes, excessive RyR2 Ca^{2+} release contributes to increased Na^{+}-Ca^{2+}-exchanger (NCX) activity which can delay plasma membrane repolarisation, the hallmark of LQTS, and sets the conditions for delayed-after-depolarisations [46,57-59]. In addition, excessive RyR2 Ca^{2+} release can in general contribute to a variety of cardiomyopathies [56,57]. Importantly, our results do not imply that CaM mutations cause LQTS via insufficient RyR2 inhibition, but rather that aberrant RyR2 Ca^{2+} release is a general underlying component of CaM-mediated arrhythmias. Understanding how several cardiac Ca^{2+}-signalling pathways are perturbed by CaM mutations has clinical implications, e.g. treating CaM-mediated LQTS using a $Ca_V1.2$-targetted approach alone may not be sufficient and may require co-treatment for the aberrant RyR2 regulation to combat CPVT. The effect of CaM mutations on RyR2 regulation in cardiac cells is difficult to delineate from effects on e.g. $Ca_V1.2$, $Na_V1.5$ and many other CaM signalling pathways, but the results presented here show such studies are well warranted [2,55-57].

EXPERIMENTAL PROCEDURES

Model Fitting and Statistical Analyses

All fitting of data to mathematical models and statistical analyses was done using GraphPad Prism 7 for Mac (version 7.0c). Models and statistical method details are described below.

Plasmids

For CaM plasmid expression in HEK293 cells, the necessary pcDNA3.1 (Thermo Fischer Scientific, Waltham, MA, USA) plasmids with the human *CALM1* cDNA insert and arrhythmogenic mutants were ordered from Genscript. A pcDNA3 (Thermo Fischer Scientific) plasmid encoding the D1ER Ca^{2+} probe was from a previous study [13,24,60]. For expression of CaM variants in *E. coli*, either pMAL (CaM-N54I, -D96V, -N98S, -D130G, -F142L) or pET15b vectors were used [5,6,61,62]. pET15b plasmids were custom-ordered and inserts DNA-synthesized (Genscript). The construction of a pcDNA5 (Thermo Fischer Scientific) plasmid carrying mouse RyR2 cDNA (pcDNA5-RyR2) has been described previously [63]. All plasmid inserts were confirmed by DNA sequencing.

Protein Expression and Purification

CaM was expressed from the pMAL or the pET15b vectors in *E. coli* Rosetta B cells (MilliPoreSigma, Burlington, MA, USA) and purified as previously described [61,62]. The identity, purity, and integrity of each protein preparation were confirmed by SDS-PAGE using intact proteins and MALDI-TOF mass spectrometry of trypsin digested proteins.

Generation of Stable and Inducible HEK293 Cell Lines

Stable inducible HEK293 cell lines expressing mouse RyR2 were generated using the pcDNA5-RyR2 plasmid with the Flp-In T-REx Core Kit (Thermo Fischer Scientific) as previously described [24]. This recombinase mediated approach integrates the RyR2 cDNA under control of a tetracycline inducible promoter into the flipase recognition target site in the HEK293 Flp-In cell line genome.

Endoplasmic Reticulum Luminal Ca^{2+} Imaging of HEK293 Cells Expressing RyR2 during Store-Overload Induced Ca^{2+} Release (SOICR)

Single cell endoplasmic reticulum (ER) luminal Ca^{2+} imaging of RyR2-expressing HEK293 cells was done as previously described [13,24,26,60]. Briefly, HEK293 cells stably expressing murine RyR2 were co-transfected with plasmids encoding CaM variants and the D1ER Ca^{2+} probe, and single cell ER luminal free Ca^{2+} concentrations (ER Ca^{2+} load) were monitored in an epi-fluorescent microscope setting using the D1ER FRET signals (Figure 2). From the single cell D1ER signals, the RyR2 Ca^{2+} release properties were measured: the activation threshold (ER Ca^{2+} load at SOICR initiation) and the termination threshold (ER Ca^{2+} load at Ca^{2+} release cessation), and their difference was the fractional ER Ca^{2+} release (change in ER Ca^{2+} load per release-reuptake cycle). The activation and termination thresholds were measured relative to the ER Ca^{2+} store capacity which was calculated from the difference between the maximum and minimum FRET signal (F_{max} - F_{min}) as obtained by perfusing with 1 mM tetracaine and 20 mM caffeine (Figure 2, box). Different CaM expression conditions were used: no plasmid expression (endogenous CaM), and pcDNA3.1 expression of each of the CaM variants. HEK293 cells do possess a ER Ca^{2+} release mechanism mediated by the inositol triphosphate

receptor, however, without RyR2-expression no Ca^{2+} oscillations or release are observed in HEK293 cells under our experimental conditions. Moreover, in experiments with expression of RyR2-ΔCaMBD, the RyR2-mediated ER Ca^{2+} oscillations are insensitive to plasmid expression of any CaM variant [5,6,13,24].

For each of the three properties (the activation and termination threshold, and the ER Ca^{2+} release) the measured values from multiple singe cell D1ER time traces were combined into one data set, and data sets from two previous studies were also considered [5,6]. The averages for each property were then compared for all possible comparisons, within each study, using one-way ANOVA with a Holm-Sidak multiple comparisons correction, $p < 0.05$ considered significant (Table 2). Using the same approach, no significant differences were identified for the comparison of ER store capacities. To directly compare the effects of different CaM expression conditions on the RyR2 Ca^{2+} release properties, a study-wise baselining was done. For each data set, all data points were subtracted the averaged value from the control (Ctrl) condition, i.e. with only endogenous CaM expression. This transformed all data sets into values of quantified changes in any given RyR2 property as conferred by plasmid expressing each of the CaM variants, relative to endogenous CaM expression (Figure 3). The quantified changes in RyR2 properties were also compared for all possible comparisons using one-way ANOVA with a Tukey multiple comparisons correction, $p < 0.05$ considered significant.

Estimation of CaM expression levels in HEK293 Cells

HEK293 cells were cultured as described above and transfected with or without CaM-WT and mutant plasmids. Cell lysates prepared from transfected cells were used for Western blotting for CaM and actin as previously described (Figure 9) [6]. The primary antibodies used were a CaM N-domain specific variant (Ab124742, Abcam, Cambridge, UK) and a generic actin antibody (A5316, MilliporeSigma). As a measure of protein expression levels, the protein band area intensities were quantified using ImageJ, and the expression levels of total CaM in individual samples were normalized to that of β-actin [6,64]. Western blot analysis was done in triplicates, and expressions levels were compared for all possible combinations using one-way ANOVA with a Tukey multiple comparisons correction, $p < 0.05$ considered significant. The double bands observed for CaM-D130V are a common artefact due to the high protein stability of Ca^{2+}-saturated CaM (details in 'Experimental procedures') and the difficulties in denaturing CaM in lysates, and even purified CaM. I.e. most CaM variants remain Ca^{2+} bound and resist denaturation during SDS-PAGE, but the D130V mutation most severely reduces free CaM's affinity for binding to Ca^{2+} and thus leaves CaM-D130G more susceptible to denaturation during sample preparation, compared to the other CaM variants [8,43,62].

Endoplasmic Reticulum Luminal Ca^{2+} Imaging of Permeabilized HEK293 Cells Expressing RyR2 with sustained 1 μM Cytosolic Ca^{2+}

Measurements of permeabilized HEK293 single cell steady-state ER Ca^{2+} load during perfusion with sustained 1 μM $[Ca^{2+}]_{free}$ was done as previously described with modifications [27,65]. Briefly, RyR2 expressing HEK293 cells were permeabilized by perfusion with 0.25 g/L saponin in Ca^{2+} free intracellular-like medium (ICM, 125 mM KCl, 19 mM NaCl, 10 mM HEPES, 2 mM ATP, 2 mM $MgCl_2$, and 50 μM EGTA at pH 7.4) for 1-2 min. The extent of permeabilization was continuously monitored and halted by switching to ICM with 0.1 μM $[Ca^{2+}]_{free}$ for another 4 min. The D1ER FRET signal from single cells was then recorded during six different perfusion conditions (Figure 4): 0.1 μM $[Ca^{2+}]_{free}$, 1 μM $[Ca^{2+}]_{free}$, 1 μM $[Ca^{2+}]_{free}$ + 0.4 μM purified CaM mutant, 1 μM $[Ca^{2+}]_{free}$ + 0.4 μM purified CaM-WT, 0.1 μM $[Ca^{2+}]_{free}$ + 1 mM tetracaine, and finally 0.1 μM $[Ca^{2+}]_{free}$ + 10 mM caffeine, all in ICM. All perfusions were done for 6 min, except for ICM with 0.1 μM $[Ca^{2+}]_{free}$ which was for 4 min. Perfusion rate was ~1.5 mL/min into an ~0.5 mL perfusion chamber. The steady-state ER Ca^{2+} load was measured as the 1 min averaged FRET signal at the end of each perfusion step, and averages were converted to ER Ca^{2+} load relative to the ER store capacity (Figure 4 and Figure 5). The effect of a CaM mutant and the CaM-WT on ER Ca^{2+} load was measured for each single cell time trace as the difference between steady-state ER Ca^{2+} load at 1 μM $[Ca^{2+}]_{free}$ without any CaM and the Ca^{2+} load after addition of purified CaM mutant and CaM-WT, respectively (Figure 4 box). Permeabilization and perfusion without Ca^{2+} washed out endogenous CaM as evident from RyR2 and RyR2-ΔCaMBD showing the same the steady-state ER Ca^{2+} load before addition of CaM, and also supported by CaM-RyR2 dissociation kinetics (Figure 5C) [21,28]. The marked response of RyR2 to exogenous CaM addition also supported endogenous CaM wash-out (Figure 4). The HEK293 cell endogenous SERCA2b operates at constant, maximum capacity under the perfusion conditions chosen, and CaM does not regulate SERCA2b as also evident from the a control experiment with RyR2-ΔCaMBD (Figure 5C) [2,27,65-67]. The differences in steady-state Ca^{2+} load with no CaM, with CaM mutant and with CaM-WT were evaluated using two-way ANOVA (CaM presence versus perfusion condition) with a Tukey's multiple comparisons correction, $p < 0.05$ considered significant. No significant differences in store capacities were identified using the same approach. Differences between the quantified effects of CaM variants on the steady-state Ca^{2+} load were compared for all possible comparisons using one-way ANOVA with a Tukey's multiple comparisons correction, $p < 0.05$ considered.

Fluorescently labelled RyR2(R3581-L3611) Peptide

A peptide (RyR2(R3581-L3611)) corresponding to the RyR2 CaMBD (human RyR2 ^{3581}RSKKAVWHKLLSKQRKRAVVACFRMAPLYNL^{3611}) with an N-terminal 5-TAMRA (5-carboxy-tetramethyl-rhodamine) label was purchased from Proteogenix (Schiltigheim, France) at > 95

% purity. Peptide concentrations were determined from the TAMRA absorption at 556 nm (extinction coefficient 103.000 $cm^{-1}M^{-1}$). Stock solutions (~600 µM) were kept in 5 % acetonitrile and 0.1 % trifluoroacetic acid.

pH- and Ca^{2+}-buffered solutions

pH- and Ca^{2+}-buffered solutions (pCa-buffer) contained 50 mM HEPES, 100 mM KCl, 0.5 mM EGTA, 1 mM free Mg^{2+} and 2 mM nitrilotriacetic acid (NTA) at pH 7.2 (25 ^{o}C) with variable concentrations of $CaCl_2$. Before dilution and pH adjustment (with ~40 mM KOH), the batch of buffer was split and one aliquot added $CaCl_2$ to 3 mM total Ca^{2+} ($[Ca^{2+}]_{tot}$). Mixing various amounts of the pCa-buffers with and without 3 mM $CaCl_2$ to different $[Ca^{2+}]_{tot}$ established defined, EGTA/NTA-buffered $[Ca^{2+}]_{free}$ [68]. In practice, x1.5 concentrated buffer stocks were prepared and protein, peptide and reducing agent (0.3 mM tris(2-carboxyethyl)phosphine (TCEP)) were added to the double distilled water used for dilution. The calculated buffer ionic strength was 156 mM, and the $[Ca^{2+}]_{free}$ was verified using the Ca^{2+} probe Fura-2 (Thermo Fischer Scientific) and binding of Ca^{2+} to free CaM or the CaM/RyR2(R3581-L3611) protein-peptide complex [5].

Titrations of the RyR2(R3581-L3611) peptide with CaM at discrete Ca^{2+} concentrations

A two-dimensional titration assay was employed to determine the affinity of CaM variants for binding to the RyR2(R3581-L3611) peptide at 16 discrete $[Ca^{2+}]_{free}$. The binding of CaM to the peptide was monitored as the change in the fluorescence anisotropy (FA) signal from the TAMRA-label. The titrations and FA measurements were done as previously described [31]. Briefly, titrations were done in 384-well microtiter plates (#3575, Corning, New York, NY, USA) with the peptide concentrations kept constant (~50 nM), and varying the CaM concentration. Using the pCa-buffers (see above) allowed for mixing high and low $[Ca^{2+}]_{tot}$ solutions to obtain specific $[Ca^{2+}]_{free}$ [68]. Each microtiter plate contained 24 titration points (CaM to peptide ratios) at each of the 16 different $[Ca^{2+}]_{free}$ (24 columns by 16 rows). CaM concentrations covered the range 0.2 nM – 18 µM, and $[Ca^{2+}]_{free}$ the range 0.3 nM – 400 µM. Immediately after mixing, the FA signal was measured in a fluorescence plate reader (Infinite M1000, Tecan, Zurich, Switzerland). Mixings and measurements were done in triplicates at 25°C.

Titration curve analysis for measuring affinity of CaM for binding to RyR2(R3581-L3611)

CaM binds the RyR2(R3581-L3611) peptide (P) stoichiometrically with the affinity for binding expressed as the protein-peptide complex's (PCaM) dissociation constant (K_D) i.e.

$$PCaM \leftrightarrows P + CaM$$

$$K_D = \frac{[P] \cdot [CaM]}{[PCaM]}$$

, where [P], [CaM] and [PCaM] are the concentrations of free peptide, CaM and complex, respectively. This simple binding model assumes one type of protein-peptide interaction characterized by one K_D, and the fractional saturation (Y) of peptide with protein is therefore given by

$$Y = \frac{[PCaM]}{[P]_{tot}} = \frac{K_D + [P]_{tot} + [CaM]_{tot}}{2 \cdot [P]_{tot}} - \sqrt{\left(\frac{K_D + [P]_{tot} + [CaM]_{tot}}{2 \cdot [P]_{tot}}\right)^2 - \frac{[CaM]_{tot}}{[P]_{tot}}} \quad (1)$$

where $[P]_{tot}$ and $[CaM]_{tot}$ are the total concentrations of peptide and CaM. For each microtiter plate row, a titration curve of FA as a function of $[CaM]_{tot}$ was measured. The FA signal consists of that from the free peptide FA (FA_P) plus that from the protein-peptide complex (FA_{PCaM}), hence

$$FA = FA_P \cdot (1 - Y) + FA_{PCaM} \cdot Y \quad (2)$$

, where FA_P and FA_{PCaM} are the minimum and maximum FA signals obtainable. Inserting equation 2 in 1 allowed for fitting the 1:1 binding model to the titration curve and thus obtaining a K_D at that $[Ca^{2+}]_{free}$. Differences between fitted K_D values, at each $[Ca^{2+}]_{free}$, were evaluated using one-way ANOVA with a Fisher's LSD test against the CaM-WT K_D, $p < 0.05$ considered significant. For statistically significant differences in K_D, the mutation induced change in standard (1 M and 25 ^oC) Gibb's free energy of binding ($\Delta\Delta G^o$) was calculated as

$$\Delta\Delta G^o = -R \cdot T \cdot \ln\left(\frac{K_{D,CaM-WT}}{K_{D,CaM-variant}}\right)$$

Estimating the CaM-Peptide Complex's Affinity for Binding to Ca^{2+}

The tripartite interaction between CaM, Ca^{2+}, and the RyR2(R3581-L3611) peptide is thermodynamically coupled and in the CaM-peptide complex, the CaM N- and C-domain have a 20- and 80-fold higher affinity for binding Ca^{2+} compared to free CaM. Also, Ca^{2+}-bound CaM has a 1200-fold higher affinity for binding to RyR2(R3581-L3611) than apoCaM [5,6,22,31]. The average K_D for the Ca^{2+}-free CaM variants binding to RyR2(R3581-L3611) is approximately 1 μM. Therefore, for conditions with 200 nM CaM and 50 nM peptide only 2-4 % would be in the CaM/RyR2(R3581-L3611) complex form. Because the equilibria between Ca^{2+}, CaM and RyR2(R3581-L3611) is strongly shifted towards formation of the Ca^{2+}-bound complex, titration of CaM in the presence of the RyR2(R3581-L3611) peptide, using the aforementioned concentrations, leads to formation of the Ca^{2+}-bound complexes with negligible Ca^{2+}-free complex. Thus, we estimated the CaM's apparent affinity for Ca^{2+} (K_{Hill}) when in complex with RyR2(R3581-L3611) by monitoring the FA change with increasing $[Ca^{2+}]_{free}$ in a 200 nM CaM to 50 nM peptide solution. These curves were fitted to a generic Hill model for Ca^{2+} binding to the protein-peptide complex [69]

$$\theta = \frac{1}{\left(\frac{K_{Hill}}{[Ca^{2+}]_{free}}\right)^n + 1}$$

, where θ is the fractional saturation of CaM/RyR2(R3581-L3611) with Ca^{2+}, n the Hill coefficient and K_{Hill} is the $[Ca^{2+}]_{free}$ where $\theta = 0.5$. Fitting was done to the raw FA signals as a function of

$[Ca^{2+}]_{free}$ with θ substituted for Y in equation 2. Differences between fitted K_{Hill} and n were evaluated for all possible combinations using one-way ANOVA with a Holm-Sidak multiple comparisons correction, $p < 0.05$ considered significant.

Bilayer Recordings of Single RyR2 Channels

Experiments were done as previously described with minor changes [6,70,71]. Native SR microsomes isolated from canine cardiac ventricles were incorporated into bilayers using a modification of the method described by Chamberlain *et al.* [72]. Briefly, planar lipid bilayers (50 g/l in a 5:4:1 mixture of bovine brain phosphatidylethanolamine, -serine, and -choline in *n*-decane) were formed across a 100-μm-diameter hole in a Teflon partition separating two compartments with cytosolic (114 mM Tris, 250 mM HEPES, 5 mM ATP, 1 mM free Mg^{2+}, 0.5 mM EGTA, and 10 μM $[Ca^{2+}]_{free}$ at pH 7.4) and luminal (cytosolic solution plus 200 mM Cs-HEPES and 1 mM $[Ca^{2+}]_{free}$ at pH 7.4) recording solutions. Single RyR2 activity was measured at +40 mV before and 20 min after the addition of CaM variants (1 μM) to the cytosolic solution [6]. Mimicking the cytosolic and intra-SR cellular milieu *in vitro* during planar lipid bilayer studies is not possible. Hence, experimental compromises were necessary, and the solutions used here approximated the cardiomyocyte cytosolic conditions during early systole. Lower cytosolic Ca^{2+} (0.1–1 μM) reduces RyR2 activity below that necessary for reliable measurements. Some researchers address this issue by omitting Mg^{2+}, but in our view this causes a highly non-physiological RyR2 Ca^{2+} dependence, as Mg^{2+} competes with Ca^{2+} for occupancy of RyR2 cytosolic Ca^{2+} activation and inactivation sites [70]. Differences in single channel parameters (P_O, MOT, and MCT) measured from time traces were compared using two-tailed, unpaired *t* tests against the average for the condition without CaM and also against the condition with CaM-WT added, $p < 0.05$ considered significant.

ACKNOWLEDGEMENTS

This study was supported by grants from the Lundbeck Foundation (2013-14432), the Novo Nordisk Foundation (NNF15OC001776299, NNF16OC0023344), the Independent Research Fund Denmark (DFF-4181-00447) and the Obelske Family Fund to MTO. And grants from the Heart and Stroke Foundation of Canada (G-16-00014214) and the Canadian Institutes of Health Research (MOP-123506) to SRWC. And a grant from the Independent Research Fund Denmark (DFF-4093-00242) to MTS.

AUTHOR CONTRIBUTIONS

MTS, YL, MB, WG, AN and CC performed experiments and analyzed the data. MTS and SRWC designed and directed the study with contributions from MF and MTO. MTS and SRWC consolidated

results across experiments, completed statistical analyses and wrote the manuscript. MF and MTO reviewed the results and revised the manuscript.

TABLES

Table 1: Arrhythmogenic CaM mutations investigated in this study. CaM is expressed from three human genes (CALM1-3) encoding identical proteins [73,74]. Previously reported functional effects of CaM mutations on the ion channels RyR2, $Na_V1.5$ and $Ca_V1.2$ are indicated using a simple annotation. CDI: CaM-mediated Ca^{2+}-dependent inactivation of $Ca_V1,2$; I_{late}: $Na_V1.5$-carried late Na^+ current. *Observed with a fetal $Na_V1.5$ splice variant.

Protein Mutation	Gene(s)	Phenotype	Effect on Ion Channel Regulation			References
			RyR2	$Na_V1.5$	$Ca_V1.2$	
F90L	*CALM1*	IVF	n/d	n/d		[75]
D96V	*CALM2*	LQTS	Less inhibition	No effect	Less CDI	[4-6,10,50]
N98I	*CALM2*	LQTS				[10,52]
N98S	*CALM2*	LQTS/CPVT	Less inhibition		Less CDI	[4-7,10,52,61]
A103V	*CALM3*	CPVT				[51]
D130V	*CALM2*	LQTS				[8]
D130G	*CALM1-3*	LQTS	Less inhibition	Increased I_{late}*	Less CDI	[4-6,8,11,50,76]
D132E	*CALM2*	LQTS/CPVT				[52]
D132H	*CALM2*	LQTS			Less CDI	[9]
D132V	*CALM1*	LQTS			Less CDI	[9]
D134H	*CALM2*	LQTS				[52]
Q136P	*CALM2*	LQTS/CPVT				[52]
E141G	*CALM1*	LQTS		Increased I_{late}		[8]
F142L	*CALM1*	LQTS	Complex effects	No effect	Less CDI	[6,8,10,50,77]

Table 2: Quantified Ca^{2+} release properties of RyR2–mediated SOICR after expression of CaM-WT or mutants. Activation and termination thresholds, and fractional ER Ca^{2+} release are given in units of % with 95 % CI in parentheses. Bold font indicates values different from those for the conditions with CaM-WT expression within each data set (one-way ANOVA with a Holm-Sidak correction, $p < 0.05$). Without CaM plasmid expression (Ctrl), HEK293 endogenous CaM remains. Results from RyR2-ΔCaMBD expressing cells are included as a reference for the ablation of CaM-dependent RyR2 inhibition. Experiments in [5] were done using a plasmid variant with a lower CaM protein yield and therefore no effect of CaM-WT plasmid expression was observed. However, data sets can be compared between studies using the shared control. The effects of CaM-N54I, -D96V, -N98S and -D130G may be slightly underestimated compared to CaM mutants in this study and [6].

CaM plasmid expression	Activation Threshold	Termination Threshold	Fractional ER Ca^{2+} Release	Single Cell Traces Analysed	Data set
(none, Ctrl)	91 (0.9)	**56** (1.7)	**34** (1.3)	121	(This study)
WT	91 (1.0)	60 (1.7)	31 (1.4)	96	(This study)
F90L	92 (0.8)	**45** (2.0)	**48** (1.9)	83	(This study)
N98I	**87** (1.4)	**44** (1.9)	**44** (2.3)	58	(This study)
A103V	92 (0.9)	**52** (2.1)	**40** (1.7)	74	(This study)
D130V	91 (1.1)	**47** (2.4)	**44** (2.2)	75	(This study)
D132E	**88** (1.3)	**35** (2.0)	**53** (2.1)	99	(This study)
D132H	90 (1.2)	**36** (2.3)	**55** (2.4)	80	(This study)
D132V	90 (1.4)	**36** (2.6)	**54** (2.5)	60	(This study)
D134H	89 (1.2)	**31** (2.3)	**58** (2.8)	60	(This study)
E141G	90 (0.8)	**35** (1.6)	**54** (1.8)	118	(This study)
Q136P	**88** (1.0)	**41** (1.8)	**47** (1.8)	143	(This study)
(none, Ctrl)	92 (1.1)	**60** (1.5)	**32** (1.4)	118	[6]
WT	93 (1.0)	64 (1.5)	30 (1.4)	90	[6]
F142L	93 (0.9)	**55** (1.6)	**38** (1.5)	142	[6]
(none, Ctrl)	91 (0.8)	57 (1.0)	34 (1.0)	193	[5]
WT	91 (1.4)	56 (1.6)	35 (1.4)	75	[5]
N54I	**86** (1.2)	**44** (1.4)	**42** (1.3)	166	[5]
D96V	**85** (2.7)	**38** (3.4)	**48** (3.0)	47	[5]
N98S	**87** (1.0)	**39** (1.3)	**48** (1.1)	178	[5]
D130G	**87** (1.7)	**40** (2.8)	**47** (2.4)	64	[5]
(RyR2-ΔCaMBD)	91 (0.7)	**34** (1.2)	**58** (1.2)	285	[5]

Table 3: Effect of CaM on steady-state ER Ca^{2+} load in permeabilized HEK293 cells expressing RyR2 and with 1 μM cytosolic $[Ca^{2+}]_{free}$. The effects on steady-state ER Ca^{2+} load of adding CaM variants to the perfusion medium, 95 % CI in parentheses (see Figure 4). All effects of CaM mutants were significantly different from the effect of CaM-WT addition and, except for CaM-F90L, -D96V, -A103V, and -F142L, also significantly different from no change in ER Ca^{2+} load (one-way ANOVA with Tukey's correction, $p < 0.05$).

CaM added	Effect on ER Ca^{2+} load (%)	Single Cell Traces Analysed
WT	13 (0.5)	483
F90L	-3 (1.2)	38
D96V	-4 (1.0)	40
N98I	-11 (1.6)	47
N98S	-9 (1.7)	25
A103V	-4 (2.0)	19
D130G	-12 (1.8)	31
D130V	-12 (1.9)	39
D132E	-11 (1.7)	38
D132H	-11 (1.4)	46
D132V	-13 (1.9)	34
D134H	-11 (2.0)	29
Q136P	-12 (1.6)	33
E141G	-7 (2.1)	19
F142L	-3 (1.3)	45

Table 4: Fitted apparent affinities (K_{Hill}) of CaM binding to Ca^{2+} when also binding RyR2(R3581-L3611). Fold change is the ratio of CaM mutant K_{Hill} to the CaM-WT K_{Hill}. The fitted Hill coefficients (n) are also shown. Values significantly different from those for the CaM-WT are in bold font (one-way ANOVA with Holm-Sidak correction, $p < 0.05$), and SD are in parentheses. For comparison, the CaM domain-wise affinity for binding Ca^{2+} ($appK_D$) determined using intrinsic CaM fluorescence and fitting to an Adair model for Ca^{2+} binding are shown [5,6].

	RyR2(R3581-L3611) FA Ca^{2+} titration (Hill model)			**CaM intrinsic fluorescence Ca^{2+} titration (Adair model) [5,6]**	
CaM variant	K_{Hill} (μM)	Fold change (-)	n (-)	N-domain $appK_D$ (μM)	C-domain $appK_D$ (μM)
WT	0.09 (0.003)		2.0 (0.1)	0.78	0.03
F90L	**0.70** (0.02)	8	2.3 (0.2)		
D96V	**0.42** (0.02)	5	2.1 (0.2)	0.48	0.14
N98I	**0.31** (0.02)	3	1.5 (0.2)		
N98S	**0.27** (0.02)	3	2.0 (0.2)	0.71	0.15
A103V	**0.25** (0.01)	3	2.1 (0.1)		
D130G	**0.81** (0.03)	9	2.0 (0.1)	0.22	4
D130V	**0.77** (0.03)	8	2.0 (0.1)		
D132E	**0.53** (0.03)	6	**2.7** (0.3)		
D132H	**0.70** (0.02)	8	2.4 (0.2)		
D132V	**0.69** (0.04)	8	2.2 (0.2)		
D134H	**0.73** (0.03)	8	1.9 (0.1)		
Q136P	**0.65** (0.02)	7	2.3 (0.2)		
E141G	**0.83** (0.02)	9	2.1 (0.1)		
F142L	**0.34** (0.02)	4	2.1 (0.2)	0.61	0.32

Table 5: Quantified single RyR2 channel conductance properties without (Ctrl) and with CaM variants. Data is given as averages (avg) with the standard error of the mean (SEM), also see Figure 8. Data for CaM-N54I, -D96V, -N98S, -D130G and -F142L from [6] are included for comparison.

Study	CaM condition	Po (-)		MOT (ms)		MCT (ms)		
		Avg	SEM	Avg	SEM	Avg	SEM	Channels (-)
This study	(none, Ctrl)	0.43	0.05	5.5	0.9	7.2	1.1	27
	WT	0.23	0.06	2.7	0.9	9.7	2.0	6
	F90L	0.33	0.06	4.2	0.6	9.8	2.3	6
	A103V	0.78	0.05	12.3	1.6	3.6	1.3	3
	Q136P	0.57	0.07	6.8	1.6	4.3	0.9	12
Søndergaard *et al.* (2016)	(none, Ctrl)	0.47	0.03	13.7	1.4	16.8	1.7	32
	WT	0.35	0.05	10.3	1.8	23.7	3.2	11
	N54I	0.43	0.07	14.1	3.9	18.3	4.2	6
	D96V	0.54	0.09	7.4	1.3	8.2	2.7	6
	N98S	0.46	0.06	6.8	1.6	8.2	1.6	6
	D130G	0.52	0.08	8.7	1.5	9.0	2.6	8
	F142L	0.18	0.02	5.3	0.6	21.7	1.9	7

REFERENCES

1 Bers DM (2002) Cardiac excitation-contraction coupling. *Nature* **415**, 198–205.
2 Sorensen AB, Søndergaard MT & Overgaard MT (2013) Calmodulin in a heartbeat. *FEBS J.* **280**, 5511–5532.
3 Gray B & Behr ER (2016) New Insights Into the Genetic Basis of Inherited Arrhythmia Syndromes. *Circulation: Cardiovascular Genetics* **9**, 569–577.
4 Limpitikul WB, Dick IE, Joshi-Mukherjee R, Overgaard MT, George AL & Yue DT (2014) Calmodulin mutations associated with long QT syndrome prevent inactivation of cardiac L-type Ca(2+) currents and promote proarrhythmic behavior in ventricular myocytes. *Journal of Molecular and cellular cardiology* **74**, 115–124.
5 Søndergaard MT, Tian X, Liu Y, Wang R, Chazin WJ, Chen SRW & Overgaard MT (2015) Arrhythmogenic Calmodulin Mutations Affect the Activation and Termination of Cardiac Ryanodine Receptor Mediated Ca2+ Release. *J Biol Chem*, jbc.M115.676627.
6 Søndergaard MT, Liu Y, Larsen KT, Nani A, Tian X, Holt C, Wang R, Wimmer R, Van Petegem F, Fill M, Chen SRW & Overgaard MT (2016) The Arrhythmogenic Calmodulin p.Phe142Leu Mutation Impairs C-domain Ca2+-binding but not Calmodulin-dependent Inhibition of the Cardiac Ryanodine Receptor. *J Biol Chem*, jbc.M116.766253.
7 Hwang H-S, Nitu FR, Yang Y, Walweel K, Pereira L, Johnson CN, Faggioni M, Chazin WJ, Laver D, George AL, Cornea RL, Bers DM & Knollmann BC (2014) Divergent regulation of ryanodine receptor 2 calcium release channels by arrhythmogenic human calmodulin missense mutants. *Circ Res* **114**, 1114–1124.
8 Boczek NJ, Gomez-Hurtado N, Ye D, Calvert ML, Tester DJ, Kryshtal DO, Hwang H-S, Johnson CN, Chazin WJ, Loporcaro CG, Shah M, Papez AL, Lau YR, Kanter R, Knollmann BC & Ackerman MJ (2016) Spectrum and Prevalence of CALM1-, CALM2-, and CALM3-Encoded Calmodulin Variants in Long QT Syndrome and Functional Characterization of a Novel Long QT Syndrome-Associated Calmodulin Missense Variant, E141G. *Circulation: Cardiovascular Genetics* **9**, 136–146.
9 Pipilas DC, Johnson CN, Webster G, Schlaepfer J, Fellmann F, Sekarski N, Wren LM, Ogorodnik KV, Chazin DM, Chazin WJ, Crotti L, Bhuiyan ZA & George AL (2016) Novel calmodulin mutations associated with congenital long qt syndrome affect calcium current in human cardiomyocytes. *Heart Rhythm*.
10 Wang K, Holt C, Lu J, Brohus M, Larsen KT, Overgaard MT, Wimmer R & Van Petegem F (2018) Arrhythmia mutations in calmodulin cause conformational changes that affect interactions with the cardiac voltage-gated calcium channel. *Proc Natl Acad Sci USA* **8**, 201808733.
11 Yin G, Hassan F, Haroun AR, Murphy LL, Crotti L, Schwartz PJ, George AL & Satin J (2014) Arrhythmogenic calmodulin mutations disrupt intracellular cardiomyocyte Ca2+ regulation by distinct mechanisms. *J Am Heart Assoc* **3**, e000996.
12 Fruen BR, Black DJ, Bloomquist RA, Bardy JM, Johnson JD, Louis CF & Balog EM (2003) Regulation of the RYR1 and RYR2 Ca2+ release channel isoforms by Ca2+-insensitive mutants of calmodulin. *Biochemistry* **42**, 2740–2747.
13 Tian X, Tang Y, Liu Y, Wang R & Chen SRW (2013) Calmodulin modulates the termination threshold for cardiac ryanodine receptor-mediated Ca2+ release. *Biochem. J.* **455**, 367–375.
14 Fearnley CJ, Roderick HL & Bootman MD (2011) Calcium signaling in cardiac myocytes. *Cold Spring Harb Perspect Biol* **3**, a004242–a004242.
15 Van Petegem F (2015) Ryanodine receptors: allosteric ion channel giants. *Journal of Molecular Biology* **427**, 31–53.
16 Chin D & Means AR (2000) Calmodulin: a prototypical calcium sensor. *Trends Cell Biol.* **10**, 322–328.
17 Yamaguchi N, Xu L, Pasek DA, Evans KE & Meissner G (2003) Molecular basis of calmodulin binding to cardiac muscle Ca(2+) release channel (ryanodine receptor). *Journal of Biological Chemistry* **278**, 23480–23486.
18 Xu L & Meissner G (2004) Mechanism of calmodulin inhibition of cardiac sarcoplasmic reticulum Ca2+ release channel (ryanodine receptor). *Biophys J* **86**, 797–804.

19 Yamaguchi N, Takahashi N, Xu L, Smithies O & Meissner G (2007) Early cardiac hypertrophy in mice with impaired calmodulin regulation of cardiac muscle Ca release channel. *J Clin Invest* **117**, 1344–1353.
20 Arnáiz-Cot JJ, Damon BJ, Zhang X-H, Cleemann L, Yamaguchi N, Meissner G & Morad M (2013) Cardiac calcium signalling pathologies associated with defective calmodulin regulation of type 2 ryanodine receptor. *J. Physiol. (Lond.)* **591**, 4287–4299.
21 Yang Y, Guo T, Oda T, Chakraborty A, Chen L, Uchinoumi H, Knowlton AA, Fruen BR, Cornea RL, Meissner G & Bers DM (2014) Cardiac myocyte Z-line calmodulin is mainly RyR2-bound, and reduction is arrhythmogenic and occurs in heart failure. *Circ Res* **114**, 295–306.
22 Lau K, Chan MMY & Van Petegem F (2014) Lobe-specific calmodulin binding to different ryanodine receptor isoforms. *Biochemistry* **53**, 932–946.
23 Søndergaard MT, Liu Y, Guo W, Wei J, Wang R, Brohus M, Overgaard MT & Chen SRW **Probing RyR2 calmodulin binding domains that mediate the action of the arrhythmogenic calmodulin N-domain mutation N54I**. Submitted to *FEBS J (FJ-18-1144.R1).*
24 Jones PP, Jiang D, Bolstad J, Hunt DJ, Zhang L, Demaurex N & Chen SRW (2008) Endoplasmic reticulum Ca2+ measurements reveal that the cardiac ryanodine receptor mutations linked to cardiac arrhythmia and sudden death alter the threshold for store-overload-induced Ca2+ release. *Biochem. J.* **412**, 171–178.
25 Breitwieser GE & Gama L (2001) Calcium-sensing receptor activation induces intracellular calcium oscillations. *Am. J. Physiol., Cell Physiol.* **280**, C1412–21.
26 Jiang D, Xiao B, Yang D, Wang R, Choi P, Zhang L, Cheng H & Chen SRW (2004) RyR2 mutations linked to ventricular tachycardia and sudden death reduce the threshold for store-overload-induced Ca2+ release (SOICR). *Proc Natl Acad Sci USA* **101**, 13062–13067.
27 Xiao Z, Guo W, Sun B, Hunt DJ, Wei J, Liu Y, Wang Y, Wang R, Jones PP, Back TG & Chen SRW (2016) Enhanced Cytosolic Ca2+ Activation Underlies a Common Defect of Central Domain Cardiac Ryanodine Receptor Mutations Linked to Arrhythmias. *J Biol Chem* **291**, 24528–24537.
28 Balshaw DM, Xu L, Yamaguchi N, Pasek DA & Meissner G (2001) Calmodulin binding and inhibition of cardiac muscle calcium release channel (ryanodine receptor). *Journal of Biological Chemistry* **276**, 20144–20153.
29 Despa S, Shui B, Bossuyt J, Lang D, Kotlikoff MI & Bers DM (2014) Junctional cleft [Ca^{2+}]i measurements using novel cleft-targeted Ca^{2+} sensors. *Circ Res* **115**, 339–347.
30 Bers DM (2008) Calcium cycling and signaling in cardiac myocytes. *Annu. Rev. Physiol.* **70**, 23–49.
31 Brohus M, Søndergaard MT, Wayne Chen SR, Van Petegem F & Overgaard MT (2019) Ca2+-dependent calmodulin binding to cardiac ryanodine receptor (RyR2) calmodulin-binding domains. *Biochem. J.* **476**, 193–209.
32 Jiang J, Zhou Y, Zou J, Chen Y, Patel P, Yang JJ & Balog EM (2010) Site-specific modification of calmodulin $Ca^2(+)$ affinity tunes the skeletal muscle ryanodine receptor activation profile. *Biochem. J.* **432**, 89–99.
33 Saucerman JJ & Bers DM (2012) Calmodulin binding proteins provide domains of local Ca2+ signaling in cardiac myocytes. *Journal of Molecular and cellular cardiology* **52**, 312–316.
34 Persechini A & Stemmer PM (2002) Calmodulin is a limiting factor in the cell. *Trends Cardiovasc. Med.* **12**, 32–37.
35 Peersen OB, Madsen TS & Falke JJ (1997) Intermolecular tuning of calmodulin by target peptides and proteins: differential effects on Ca2+ binding and implications for kinase activation. *Protein Sci* **6**, 794–807.
36 Theoharis NT, Sorensen BR, Theisen-Toupal J & Shea MA (2008) The neuronal voltage-dependent sodium channel type II IQ motif lowers the calcium affinity of the C-domain of calmodulin. *Biochemistry* **47**, 112–123.
37 Evans TIA, Hell JW & Shea MA (2011) Thermodynamic linkage between calmodulin domains binding calcium and contiguous sites in the C-terminal tail of Ca(V)1.2. *Biophys. Chem.* **159**, 172–187.
38 Maximciuc AA, Putkey JA, Shamoo Y & Mackenzie KR (2006) Complex of calmodulin with a ryanodine receptor target reveals a novel, flexible binding mode. **14**, 1547–1556.

39 Chattopadhyaya R, Meador WE, Means AR & Quiocho FA (1992) Calmodulin structure refined at 1.7 A resolution. *Journal of Molecular Biology* **228**, 1177–1192.
40 Elshorst B, Hennig M, Försterling H, Diener A, Maurer M, Schulte P, Schwalbe H, Griesinger C, Krebs J, Schmid H, Vorherr T & Carafoli E (1999) NMR solution structure of a complex of calmodulin with a binding peptide of the Ca2+ pump. *Biochemistry* **38**, 12320–12332.
41 Fallon JL, Halling DB, Hamilton SL & Quiocho FA (2005) Structure of calmodulin bound to the hydrophobic IQ domain of the cardiac Ca(v)1.2 calcium channel. **13**, 1881–1886.
42 Jones PP, Guo W & Chen SRW (2017) Control of cardiac ryanodine receptor by sarcoplasmic reticulum luminal Ca(2). *J. Gen. Physiol.* **268**, jgp.201711805.
43 Vassilakopoulou V, Calver BL, Thanassoulas A, Beck K, Hu H, Buntwal L, Smith A, Theodoridou M, Kashir J, Blayney L, Livaniou E, Nounesis G, Anthony Lai F & Nomikos M (2015) Distinctive malfunctions of calmodulin mutations associated with heart RyR2-mediated arrhythmic disease. *Biochim Biophys Acta*.
44 Nomikos M, Thanassoulas A, Beck K, Vassilakopoulou V, Hu H, Calver BL, Theodoridou M, Kashir J, Blayney L, Livaniou E, Rizkallah P, Nounesis G & Lai FA (2014) Altered RyR2 regulation by the calmodulin F90L mutation associated with idiopathic ventricular fibrillation and early sudden cardiac death. *FEBS Lett* **588**, 2898–2902.
45 Du GG, Imredy JP & MacLennan DH (1998) Characterization of recombinant rabbit cardiac and skeletal muscle Ca2+ release channels (ryanodine receptors) with a novel [3H]ryanodine binding assay. *Journal of Biological Chemistry* **273**, 33259–33266.
46 Priori SG & Chen SRW (2011) Inherited dysfunction of sarcoplasmic reticulum Ca2+ handling and arrhythmogenesis. *Circ Res* **108**, 871–883.
47 Xie L-H, Sato D, Garfinkel A, Qu Z & Weiss JN (2008) Intracellular Ca alternans: coordinated regulation by sarcoplasmic reticulum release, uptake, and leak. *Biophys J* **95**, 3100–3110.
48 Chen W, Wang R, Chen B, Zhong X, Kong H, Bai Y, Zhou Q, Xie C, Zhang J, Guo A, Tian X, Jones PP, O'Mara ML, Liu Y, Mi T, Zhang L, Bolstad J, Semeniuk L, Cheng H, Zhang J, Chen J, Tieleman DP, Gillis AM, Duff HJ, Fill M, Song L-S & Chen SRW (2014) The ryanodine receptor store-sensing gate controls Ca(2+) waves and Ca(2+)-triggered arrhythmias. **20**, 184–192.
49 Tang Y, Tian X, Wang R, Fill M & Chen SRW (2012) Abnormal termination of Ca2+ release is a common defect of RyR2 mutations associated with cardiomyopathies. *Circ Res* **110**, 968–977.
50 Crotti L, Johnson CN, Graf E, De Ferrari GM, Cuneo BF, Ovadia M, Papagiannis J, Feldkamp MD, Rathi SG, Kunic JD, Pedrazzini M, Wieland T, Lichtner P, Beckmann B-M, Clark T, Shaffer C, Benson DW, Kääb S, Meitinger T, Strom TM, Chazin WJ, Schwartz PJ & George AL (2013) Calmodulin mutations associated with recurrent cardiac arrest in infants. *Circulation* **127**, 1009–1017.
51 Gomez-Hurtado N, Boczek NJ, Kryshtal DO, Johnson CN, Sun J, Nitu FR, Cornea RL, Chazin WJ, Calvert ML, Tester DJ, Ackerman MJ & Knollmann BC (2016) Novel CPVT-Associated Calmodulin Mutation in CALM3 (CALM3-A103V) Activates Arrhythmogenic Ca Waves and Sparks. *Circ Arrhythm Electrophysiol* **9**.
52 Makita N, Yagihara N, Crotti L, Johnson CN, Beckmann BM, Roh MS, Shigemizu D, Lichtner P, Ishikawa T, Aiba T, Homfray T, Behr ER, Klug D, Denjoy I, Mastantuono E, Theisen D, Tsunoda T, Satake W, Toda T, Nakagawa H, Tsuji Y, Tsuchiya T, Yamamoto H, Miyamoto Y, Endo N, Kimura A, Ozaki K, Motomura H, Suda K, Tanaka T, Schwartz PJ, Meitinger T, Kaab S, Guicheney P, Shimizu W, Bhuiyan ZA, Watanabe H, Chazin WJ & George AL (2014) Novel Calmodulin Mutations Associated With Congenital Arrhythmia Susceptibility. *Circulation: Cardiovascular Genetics* **7**, 466–474.
53 Zhou Q, Xiao J, Jiang D, Wang R, Vembaiyan K, Wang A, Smith CD, Xie C, Chen W, Zhang J, Tian X, Jones PP, Zhong X, Guo A, Chen H, Zhang L, Zhu W, Yang D, Li X, Chen J, Gillis AM, Duff HJ, Cheng H, Feldman AM, Song L-S, Fill M, Back TG & Chen SRW (2011) Carvedilol and its new analogs suppress arrhythmogenic store overload-induced Ca2+ release. **17**, 1003–1009.
54 Jiang D, Wang R, Xiao B, Kong H, Hunt DJ, Choi P, Zhang L & Chen SRW (2005) Enhanced store overload-induced Ca2+ release and channel sensitivity to luminal Ca2+ activation are

common defects of RyR2 mutations linked to ventricular tachycardia and sudden death. *Circ Res* **97**, 1173–1181.
55 Jensen HH, Brohus M, Nyegaard M & Overgaard MT (2018) Human Calmodulin Mutations. *Front Mol Neurosci* **11**, 396.
56 Landstrom AP, Dobrev D & Wehrens XHT (2017) Calcium Signaling and Cardiac Arrhythmias. *Circ Res* **120**, 1969–1993.
57 Bers DM (2014) Cardiac sarcoplasmic reticulum calcium leak: basis and roles in cardiac dysfunction. *Annu. Rev. Physiol.* **76**, 107–127.
58 Wehrens XHT (2007) Leaky ryanodine receptors cause delayed afterdepolarizations and ventricular arrhythmias. *Eur Heart J* **28**, 1054–1056.
59 Koivumäki JT, Korhonen T & Tavi P (2011) Impact of sarcoplasmic reticulum calcium release on calcium dynamics and action potential morphology in human atrial myocytes: a computational study. *PLoS Comp Biol* **7**, e1001067.
60 Palmer AE, Jin C, Reed JC & Tsien RY (2004) Bcl-2-mediated alterations in endoplasmic reticulum Ca2+ analyzed with an improved genetically encoded fluorescent sensor. *Proc Natl Acad Sci USA* **101**, 17404–17409.
61 Nyegaard M, Overgaard MT, Søndergaard MT, Vranas M, Behr ER, Hildebrandt LL, Lund J, Hedley PL, Camm AJ, Wettrell G, Fosdal I, Christiansen M & Børglum AD (2012) Mutations in calmodulin cause ventricular tachycardia and sudden cardiac death. *Am. J. Hum. Genet.* **91**, 703–712.
62 Søndergaard MT, Sorensen AB, Skov LL, Kjaer-Sorensen K, Bauer MC, Nyegaard M, Linse S, Oxvig C & Overgaard MT (2015) Calmodulin mutations causing catecholaminergic polymorphic ventricular tachycardia confer opposing functional and biophysical molecular changes. *FEBS J.* **282**, 803–816.
63 Zhao M, Li P, Li X, Zhang L, Winkfein RJ & Chen SR (1999) Molecular identification of the ryanodine receptor pore-forming segment. *Journal of Biological Chemistry* **274**, 25971–25974.
64 Schneider CA, Rasband WS & Eliceiri KW (2012) NIH Image to ImageJ: 25 years of image analysis. *Nat. Methods* **9**, 671–675.
65 Liu Y, Sun B, Xiao Z, Wang R, Guo W, Zhang JZ, Mi T, Wang Y, Jones PP, Van Petegem F & Chen SRW (2015) Roles of the NH2-terminal Domains of Cardiac Ryanodine Receptor in Ca2+ Release Activation and Termination. *J Biol Chem* **290**, 7736–7746.
66 Geiger T, Wehner A, Schaab C, Cox J & Mann M (2012) Comparative proteomic analysis of eleven common cell lines reveals ubiquitous but varying expression of most proteins. *Mol. Cell Proteomics* **11**, M111.014050.
67 Lytton J, Westlin M, Burk SE, Shull GE & MacLennan DH (1992) Functional comparisons between isoforms of the sarcoplasmic or endoplasmic reticulum family of calcium pumps. *Journal of Biological Chemistry* **267**, 14483–14489.
68 Dweck D, Reyes-Alfonso A & Potter JD (2005) Expanding the range of free calcium regulation in biological solutions. *Anal Biochem* **347**, 303–315.
69 Hill AV (1910) *The possible effects of the aggregation of the molecules of hæmoglobin on its dissociation curves*. *J. Physiol. (Lond.)* **40**, i–vii.
70 Qin J, Valle G, Nani A, Chen H, Ramos-Franco J, Nori A, Volpe P & Fill M (2009) Ryanodine receptor luminal Ca2+ regulation: swapping calsequestrin and channel isoforms. *Biophys J* **97**, 1961–1970.
71 Tan Z, Xiao Z, Wei J, Zhang J, Zhou Q, Smith CD, Nani A, Wu G, Song L-S, Back TG, Fill M & Chen SRWW (2016) Nebivolol Suppresses Cardiac Ryanodine Receptor Mediated Spontaneous Ca2+ Release and Catecholaminergic Polymorphic Ventricular Tachycardia. *Biochem. J.*, BCJ20160620.
72 Chamberlain BK, Volpe P & Fleischer S (1984) Calcium-induced calcium release from purified cardiac sarcoplasmic reticulum vesicles. General characteristics. *Journal of Biological Chemistry* **259**, 7540–7546.
73 Berchtold MW, Egli R, Rhyner JA, Hameister H & Strehler EE (1993) Localization of the human bona fide calmodulin genes CALM1, CALM2, and CALM3 to chromosomes 14q24-q31, 2p21.1-p21.3, and 19q13.2-q13.3. *Genomics* **16**, 461–465.
74 Friedberg F & Rhoads AR (2001) Evolutionary Aspects of Calmodulin. *IUBMB Life* **51**, 215–221.

75 Marsman RF, Barc J, Beekman L, Alders M, Dooijes D, van den Wijngaard A, Ratbi I, Sefiani A, Bhuiyan ZA, Wilde AAM & Bezzina CR (2014) A mutation in CALM1 encoding calmodulin in familial idiopathic ventricular fibrillation in childhood and adolescence. *J Am Coll Cardiol* **63**, 259–266.
76 Reed GJ, Boczek NJ, Etheridge SP & Ackerman MJ (2015) CALM3 mutation associated with long QT syndrome. *Heart Rhythm* **12**, 419–422.
77 Rocchetti M, Sala L, Dreizehnter L, Crotti L, Sinnecker D, Mura M, Pane LS, Altomare C, Torre E, Mostacciuolo G, Severi S, Porta A, De Ferrari GM, George AL, Schwartz PJ, Gnecchi M, Moretti A & Zaza A (2017) Elucidating arrhythmogenic mechanisms of long-QT syndrome CALM1-F142L mutation in patient-specific induced pluripotent stem cell-derived cardiomyocytes. *Cardiovasc Res* **113**, 531–541.

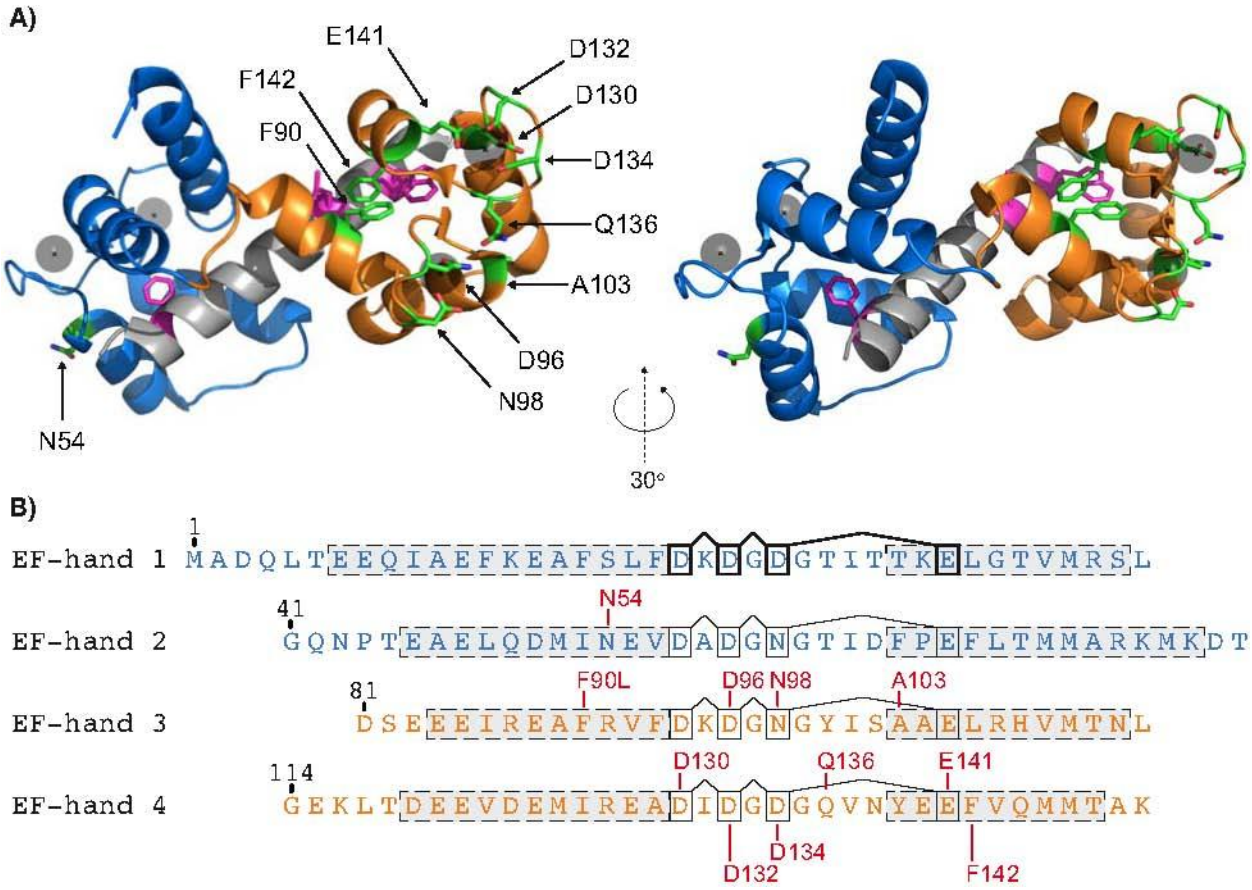

Figure 1: **A representative structure of CaM**. **A)** Ca^{2+}-saturated CaM is shown binding a 27-residue peptide corresponding to the RyR1 CaMBD (Lys-3614 to Pro-3640) (PDB file **2BCX**). Protein and peptide secondary structures are shown as cartoon representation with the CaM N-domain (Met-1 – Thr-80) in blue, the C-domain (Asp-81 to Lys-148) in orange, and the peptide in grey. CaM mutation sites are highlighted as stick representations, and Ca^{2+} ions are shown as semi-transparent, black spheres. The RyR1 CaMBD sequence differs from the RyR2 CaMBD only at Lys-3614 (RyR2 Arg-3581) and Thr-3639 (RyR2 Ala-3606). The RyR1 CaMBD residues corresponding to RyR2 CaMBD residues Trp-3587, Leu-3591, and Phe-3603 are highlighted as magenta stick representations. **B)** The four Ca^{2+} binding EF-hand motifs in CaM (UniProtKB accession **P0DP23**) manually aligned by their Ca^{2+}-coordinating residues and with the mutation sites highlighted in red. Connected boxes highlight the Ca^{2+}-coordinating residues, and grey dash-boxes denote α-helical regions.

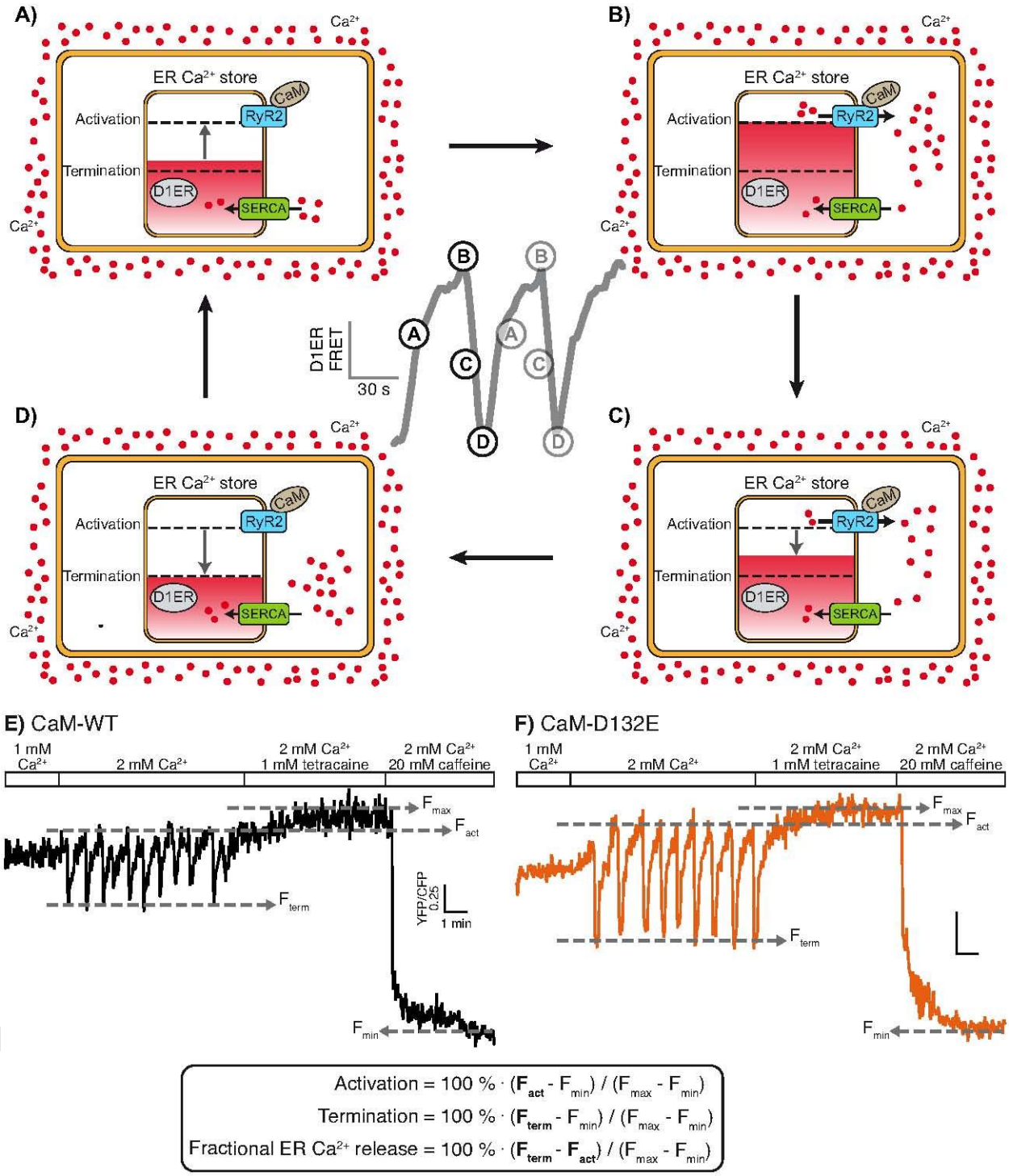

Figure 2: **SOICR in RyR2-expressing HEK293 cells transfected with CaM-WT or mutants**. Experimental principle (top): High extracellular Ca^{2+} (2 mM) increases the ER Ca^{2+} load (**A**) and ultimately causes RyR2 to open (**B**), i.e. initiation of SOICR, and release ER-stored Ca^{2+} (**C**). At a sufficiently depleted ER Ca^{2+} load, the RyR2 channels close i.e. terminate Ca^{2+} release (**D**), and ER Ca^{2+} is replenished until the ER Ca^{2+} load for SOICR is reached again (**A**). Thus, the ER Ca^{2+} load continuously oscillates with the concerted opening and closing of RyR2 (bottom): examples of cell D1ER FRET time traces from single cells expressing CaM-WT **(E)**, and cells expressing CaM-D132E **(F)**. Concentrations of extracellular Ca^{2+}, tetracaine and caffeine in the perfusion solution are shown

above the traces. Tetracaine and caffeine were used to establish maximum and minimum ER Ca^{2+} load (F_{max} and F_{min}), respectively. From each single cell time trace, three RyR2 Ca^{2+} release properties were calculated relative to F_{max} and F_{min}: the activation threshold, the termination threshold, and the fractional ER Ca^{2+} release (bottom box).

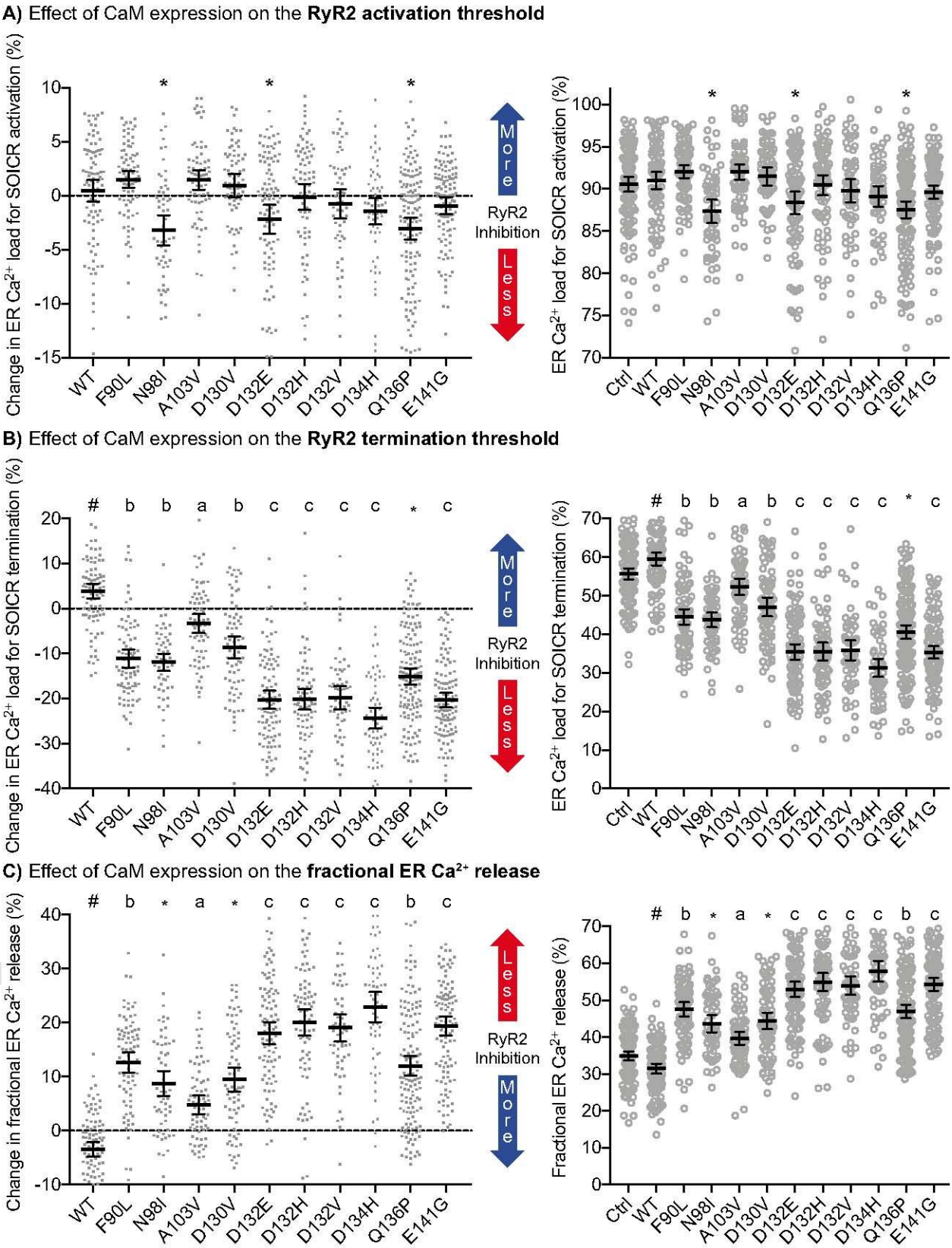

Figure 3: **Effects of CaM expression on the RyR2 Ca^{2+} release properties during SOICR in HEK293 cells**. Left hand panels are averages for the measured changes in the activation threshold (**A**), the termination threshold (**B**) and the fractional ER Ca^{2+} release (**C**) as conferred by each CaM variant (x-axis labels) as compared to the control condition with only endogenous CaM (dashed line).

The raw data points, used to calculate the changes in each RyR2 Ca^{2+} release property, are plotted in the right-hand panels of A, B, and C. Letters (a, b or c) indicate groups of averages significantly different from all other groups. Asterisks (*) indicate values significantly different from the effect of CaM-WT expression and the control. For (B) and (C) asterisks additionally indicate values not uniquely assigned to groups a or b, but still different from c. Hash (#) indicates CaM-WT averages different from the control (one-way ANOVA with Tukey's post hoc test for all possible combinations, $p < 0.05$). Error bars show the 95 % confidence interval (CI). Further data are also shown in Table 2.

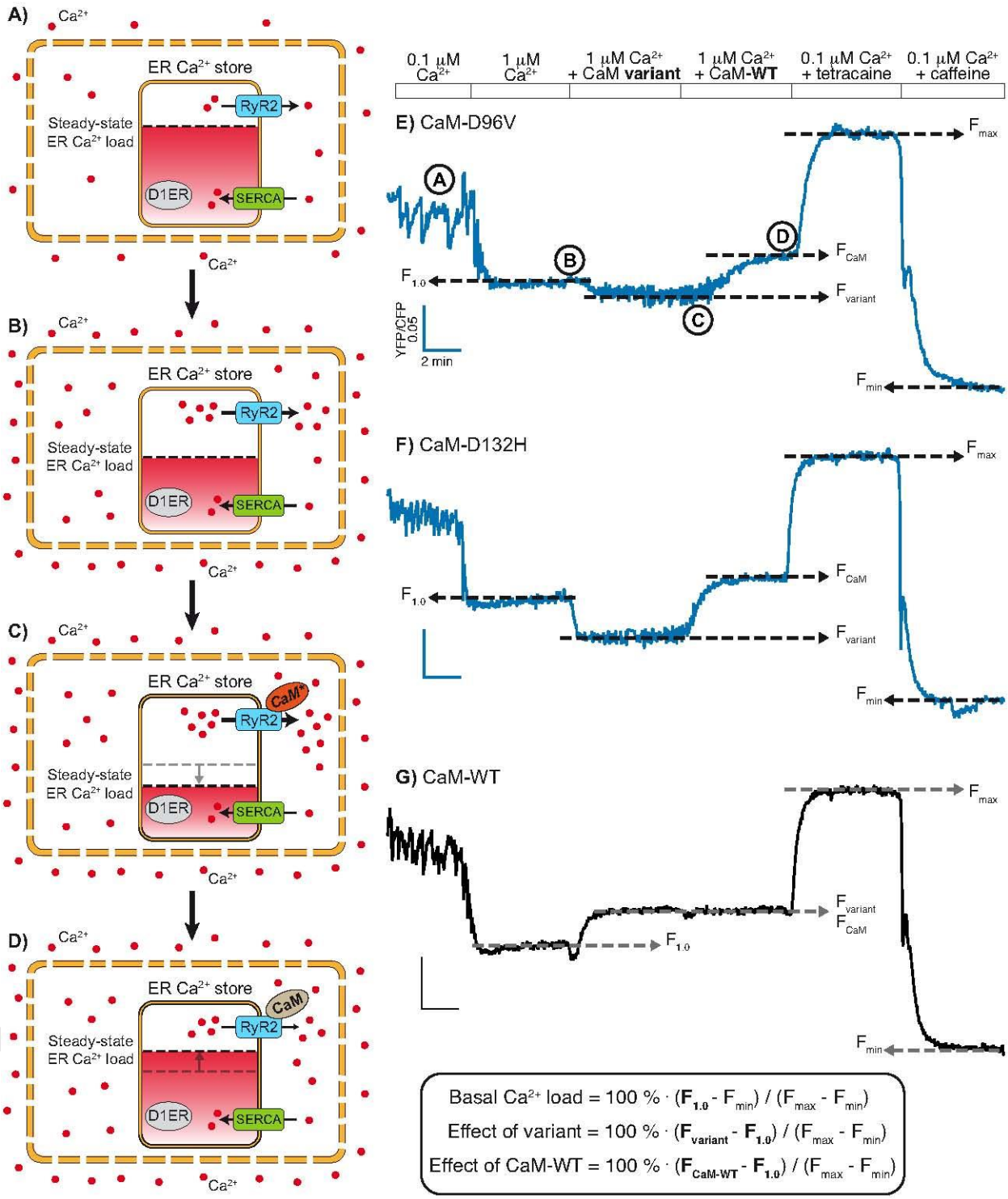

Figure 4: **Ca^{2+} release in permeabilized RyR2-expressing HEK293 cells**. Experiment principle (left): Permeabilization and perfusion washes out endogenous CaM and the continuous ER Ca^{2+} release (RyR2) and Ca^{2+} uptake (SERCA2b) establishes steady-state ER Ca^{2+} load, initially with 0.1 µM $[Ca^{2+}]_{free}$ (**A**). Increasing $[Ca^{2+}]_{free}$ to 1 µM stimulates RyR2 Ca^{2+} release and lowers ER Ca^{2+} load (**B**). Addition of CaM mutants promote RyR2 Ca^{2+} release to various extents and therefore decreases ER Ca^{2+} load (**C**), and addition of CaM-WT strongly inhibits RyR2 and thereby increases ER Ca^{2+} load (**D**). **E-G**) Examples of D1ER FRET signal time traces from permeabilized cells expressing

RyR2 (4-6 averaged) and perfused with 1 μM cytosolic Ca^{2+} and CaM as indicated above the traces. Tetracaine (1 mM) and caffeine (20 mM) were used to establish maximum and minimum ER Ca^{2+} load (F_{max} and F_{min}), respectively. Steady-state ER Ca^{2+} load at 1 μM $[Ca^{2+}]_{free}$ was calculated as the average FRET signal, relative to $F_{max} - F_{min}$, during perfusion without ($F_{1.0}$), with a CaM mutant (F_{mutant}) and then with CaM-WT added ($F_{CaM\text{-}WT}$). The quantified effects of the CaM mutants and -WT were calculated as the differences $F_{Mutant} - F_{1.0}$ and $F_{CaM\text{-}WT} - F_{1.0}$, respectively.

A) Quantified effect of CaM on the **steady-state ER Ca^{2+} load** in permeabilized HEK293 cells

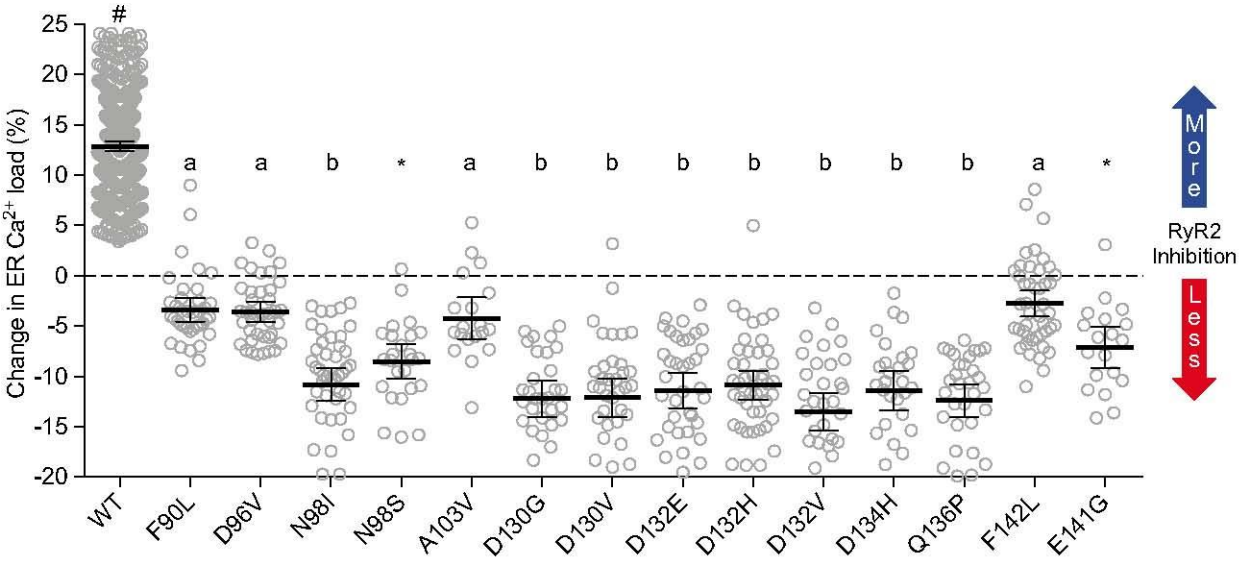

B) Steady-state ER Ca^{2+} load in permeabilized HEK293 cells during perfusion with 1 μM $[Ca^{2+}]_{free}$ and different CaM conditions

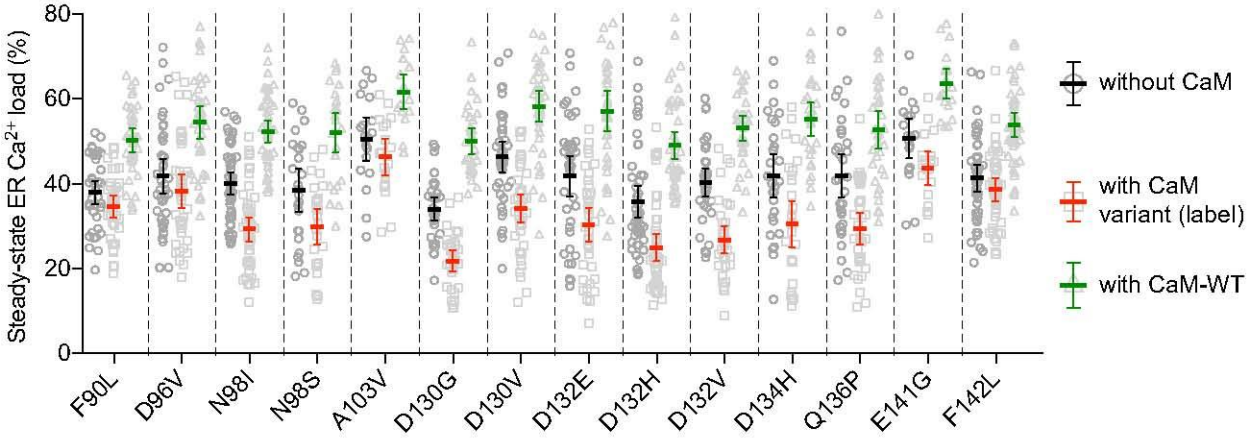

C) Effect of CaM-WT on the steady-state ER Ca^{2+} load in permeabilized RyR2- or RyR2-ΔCaMBD-expressing HEK293 cells

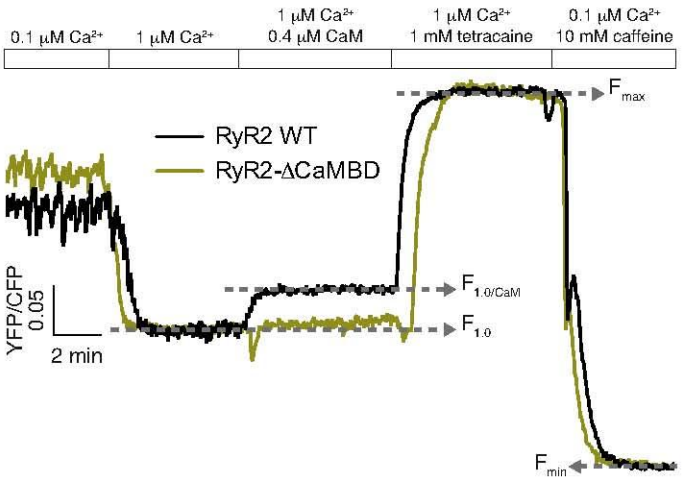

Figure 5: **Effect of CaM on steady-state Ca^{2+} load. A)** Quantified effect of CaM on steady-state Ca^{2+} load in the presence of 1 μM cytosolic $[Ca^{2+}]_{free}$ in permeabilized HEK293 cells. Averages show measured effects on ER Ca^{2+} load of adding CaM variants to the perfusion solution. a, b or c indicate groups of values significantly different from all other values, except for those within their own group (one-way ANOVA with Tukey's post hoc test for all possible combinations, $p < 0.05$). Asterisks indicate values significantly different from the effect of CaM-WT, yet not statistically distinguishable from groups a or b. Data are also summarised in Table 3. Error bars show 95 % CI. **B)** Overview of steady-state ER Ca^{2+} load measured in permeabilised, RyR2-expressing HEK293 cells. Averages for the three CaM conditions, all with 1 μM cytosolic $[Ca^{2+}]_{free}$, were calculated from multiple single cell traces (see details in Table 3). Error bars show 95 % CI. **C**) Examples of D1ER FRET time traces used for measuring the effect on the ER Ca^{2+} load from supplementing CaM-WT to RyR2 (black) or RyR2-ΔCaMBD (green).

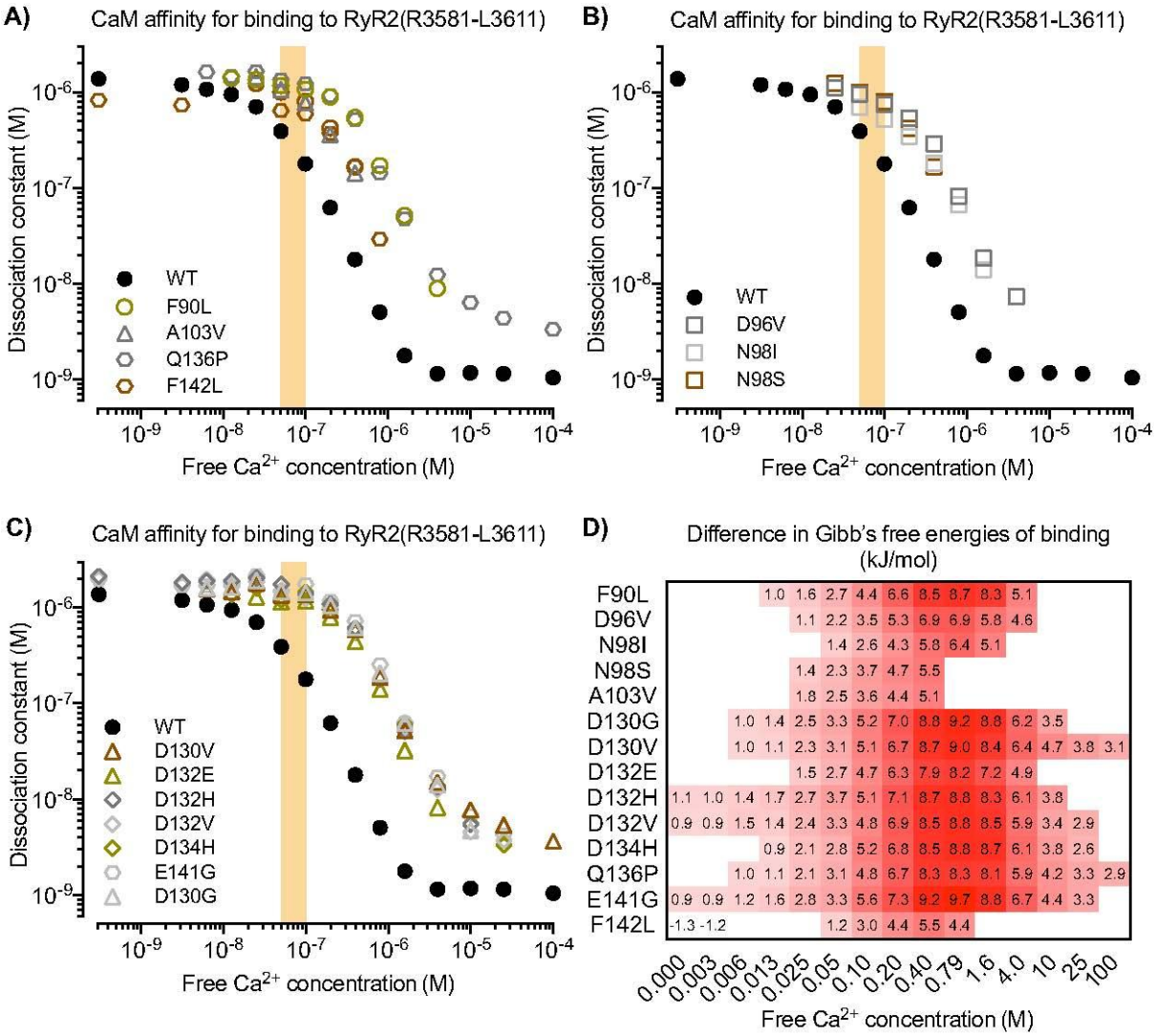

Figure 6: **Ca^{2+}-dependent affinities of CaM variants for binding to the RyR2 (R3581-L3611) peptide**. **A-C)** The binding model fitted dissociation constants (K_D) are plotted as a function of $[Ca^{2+}]_{free}$, note the double logarithmic axes. Only K_D values significantly different from those for the CaM-WT are shown (one-way ANOVA with Fisher's LSD test, $p < 0.05$). Measurements were done in triplicate. For overview purposes, plots are in several panels: mutations in **A**) none-Ca^{2+} coordinating residues, **B**) EF-hand 3 Ca^{2+}-coordinating residues, and **C**) EF-hand 4 Ca^{2+}-coordinating residues. Background shading indicates approximate cardiomyocyte diastole $[Ca^{2+}]_{cyt}$. **D)** Effects of CaM mutations on binding to the RyR2 CaMBD quantified as the difference in Gibb's free energies of binding ($\Delta\Delta G^o$). Heat map shows the $\Delta\Delta G^o$ magnitude for each CaM mutant across the $[Ca^{2+}]_{free}$ range where significant changes in K_D were observed.

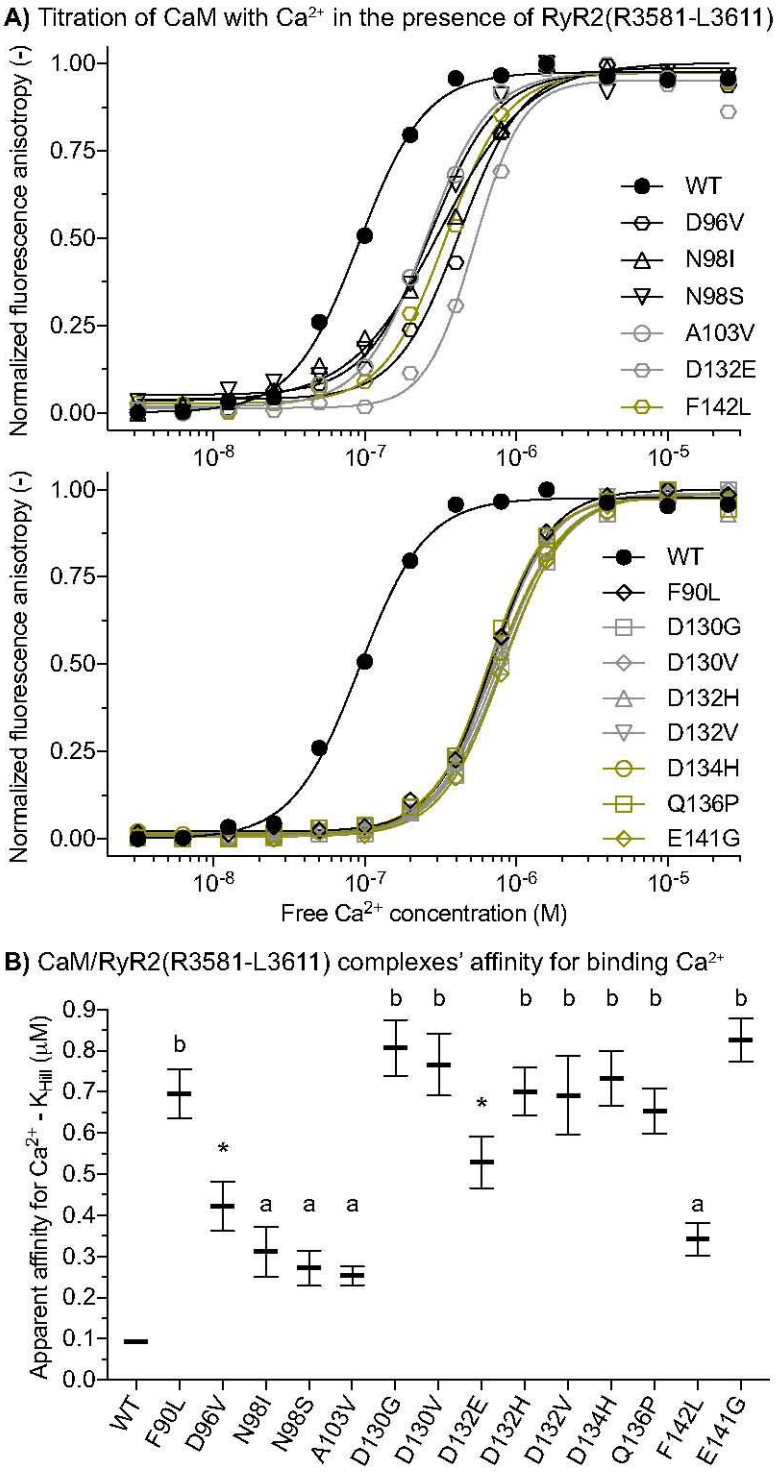

Figure 7: **CaM affinity for binding Ca^{2+} in the presence of the RyR2(R3581-L3611) peptide. A)** Ca^{2+} titration curves (FA as a function of $[Ca^{2+}]_{free}$) shown for the constant concentrations of 200 nM CaM and 50 nM RyR2(R3581-L3611) peptide. Curves were normalized for comparison purposes only, and model fitting was done using raw data. Solid lines show the Hill model fit for estimating apparent affinity for binding Ca^{2+} (K_{Hill}). Points are averages from two replicates, and bars show SD if not covered by symbol. **B)** Comparison of the K_{Hill} fitted for each CaM variant. Error bars show 95 % CI, and letters (a or b) indicate values significantly different from all others, except within their own

group. Asterisks (*) indicate values significantly different from CaM-WT, yet not uniquely distinguishable from groups a or b (one-way ANOVA with Holm-Sidak's correction, $p < 0.05$). Measurements were done in triplicate.

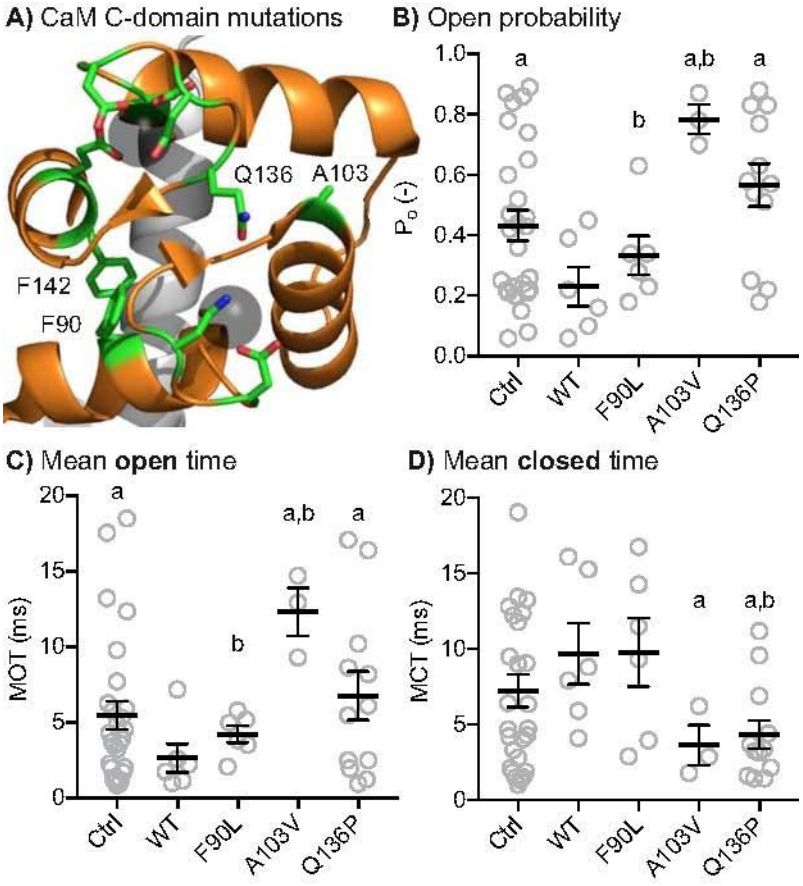

Figure 8: **Effect of CaM on the activity of single RyR2 channels. A**) Magnified view of the interface between EF-hand 3 and 4 in the CaM C-domain. The example structure is the same as in Figure 1. Amino acids affected by arrhythmogenic mutations are highlighted as stick representation, and those that are part of the EF-hand 3 and 4 interface are labelled. **B)** RyR2 channel open probability (P_o), **C**) mean open time (MOT) and **D**) mean closed time (MCT) were measured from single RyR2 channel current recordings before (Ctrl) and after the addition of 1 µM CaM. **E)** Example single RyR2 channel current traces without CaM (Ctrl) and after the addition of each of the CaM variants. Measurements were done with 1 mM $[Ca^{2+}]_{free}$ at the luminal face, and 10 µM $[Ca^{2+}]_{free}$, 1 mM free Mg^{2+} and 5 mM total ATP at the cytosolic face. Error bars indicate standard error of the mean. a indicates values significantly different from CaM-WT addition, and b indicates values significantly different from the Ctrl (t-test, $p < 0.05$). Data are also summarised in Table 5.

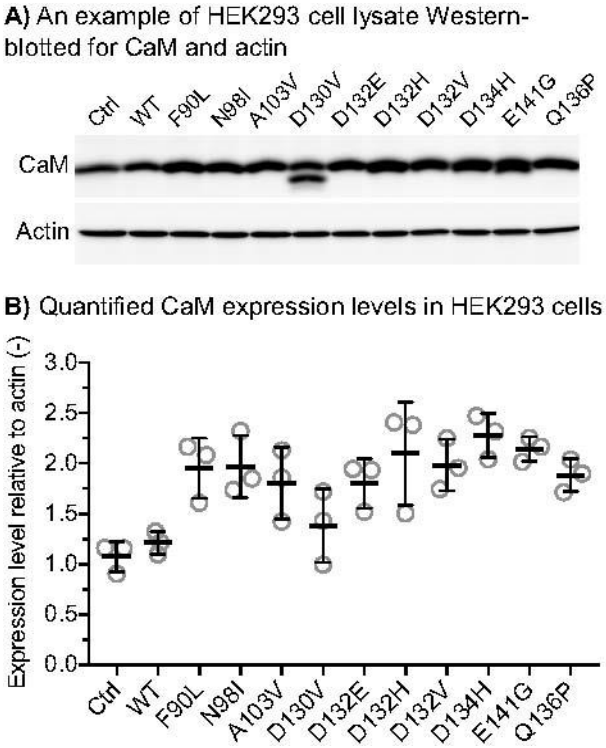

Figure 9: **Estimation of CaM expression levels in HEK293 cells. A)** Example of Western-blotted protein bands visualized using chemiluminescence imaging. HEK293 cells were cultured without (Ctrl) and with CaM plasmid expression. HEK293 cells endogenously express CaM-WT (i.e.Ctrl). **B)** Expression levels of CaM were normalized to that of β-actin. The two bands observed for CaM-D130V are an artefact due to Ca^{2+}-saturated CaM's protein stability (details in 'Experimental procedures'). No significant differences between the CaM protein levels in samples with plasmid expression of mutant variants were observed. However, the CaM protein level in samples with CaM-WT plasmid expression was significantly lower, compared to the samples with mutant CaM expression, and not significantly different from the control without plasmid expression (one-way ANOVA with Tukey's correction, $p < 0.05$).